Operations Research Perspectives 9 (2022) 100235

Contents lists available at ScienceDirect

Operations Research Perspectives

journal homepage: www.elsevier.com/locate/orp

Multi-stage stochastic optimization of islanded utility-microgrids design after natural disasters

Rodney Kizito [a,b], Zeyu Liu [a], Xueping Li [a,*], Kai Sun [c]

[a] Department of Industrial and Systems Engineering, The University of Tennessee at Knoxville, Knoxville, TN 37996, United States
[b] Solar Energy Technologies Office (SETO), Department of Energy, Washington, DC, United States
[c] Department of Electrical Engineering and Computer Science, The University of Tennessee at Knoxville, Knoxville, TN 37996, United States

ARTICLE INFO

Keywords:
Disaster relief power
Critical load restoration
Microgrid reliability
Multi-stage stochastic programming
Solar power
Energy storage system

ABSTRACT

Natural disasters (e.g., hurricanes) can cause widespread power outages within distribution networks and interrupted power supply to critical loads (e.g., grocery stores, hospitals, gas, fire, and police stations) that provide utility services. Microgrids are localized power grids that can incorporate solar/photovoltaic (PV) distributed generators (PV-DGs) and energy storage systems (ESSs) for stand-alone system operations independent of the main grid, known as the island mode. This study investigates a microgrid design problem using PV-DGs and ESSs when facing prolonged power outages in the main grid. We propose a multi-stage stochastic program that holistically considers the techno-economics of microgrid investment and daily operations by optimizing the reliability and resilience of the microgrid during a week-long power outage. The model is designed from a utility perspective that includes budget constraints for investment. Due to the large model size, we develop a nested L-shaped algorithm that solves the problem exactly and analyzes the microgrid's reliability across different weather scenarios in the entire decision-making horizon. Results from a case study using real-world data show that an islanded utility-scale microgrid can effectively provide uninterrupted power supply to a network of 5 and 10 critical loads, covering 100% and 97% of the demand in all possible future scenarios, with potential investments of $8 million and $15 million, respectively.

1. Introduction

1.1. Background

Various US cities and towns experience annual seasons of natural disasters, which can unfortunately lead to widespread outages within utility power grid networks [1]. These outages have lasted hours, days, or even weeks and left the utility's serviced population without access to critical loads such as grocery stores for food, hospitals for healthcare, gas stations for travel, and police and fire stations for protection. Microgrids serve as a subsystem of the main power grid with the ability to operate either connected to or islanded from the grid. Microgrids can consist of distributed generation, energy storage, demand nodes such as the critical loads of a city or town, a point of common coupling where the connection/disconnection of the microgrid from the main occurs, and some form of energy management systems.

Prolonged power outages have occurred in US cities and towns due to natural disaster occurrences. This reality has helped highlight how damaging natural disasters can be to the main grid [2]. The past 20 years have multiple examples of such damage. For example, Hurricane Sandy left over 285,000 New York residents powerless for two weeks. Sandy also forced 300 patients to be evacuated when a major hospital's power, provided by a utility on the main grid, was cut off, and the back-up generators of the hospital failed [3]. Other hospitals across the US have experienced similar situations after a natural disasters occurrence [4–7], with causalities witnessed in some cases [8].

Utility-scale adoption of microgrids has been a slow process due to several factors, including interconnection policy issues and regulatory challenges where utilities fear that microgrids will disrupt the business model utilities have operated under for decades [9]. However, microgrids provide several benefits for utilities and should be viewed as an opportunity and not a threat by utilities. In worst-case scenarios, such as widespread, long-term power outages, microgrids can provide reliable power supply to critical loads within a utility's serviced network [10]. With a normally functioning main grid, microgrids provide even more benefits to utilities. During normal times, microgrids can help reduce demand on the grid, especially during times of peak demand. Microgrids also help improve the energy efficiency of the grid

* Corresponding author.
E-mail address: Xueping.Li@utk.edu (X. Li).

https://doi.org/10.1016/j.orp.2022.100235
Received 13 December 2021; Received in revised form 23 March 2022; Accepted 1 April 2022
Available online 9 April 2022

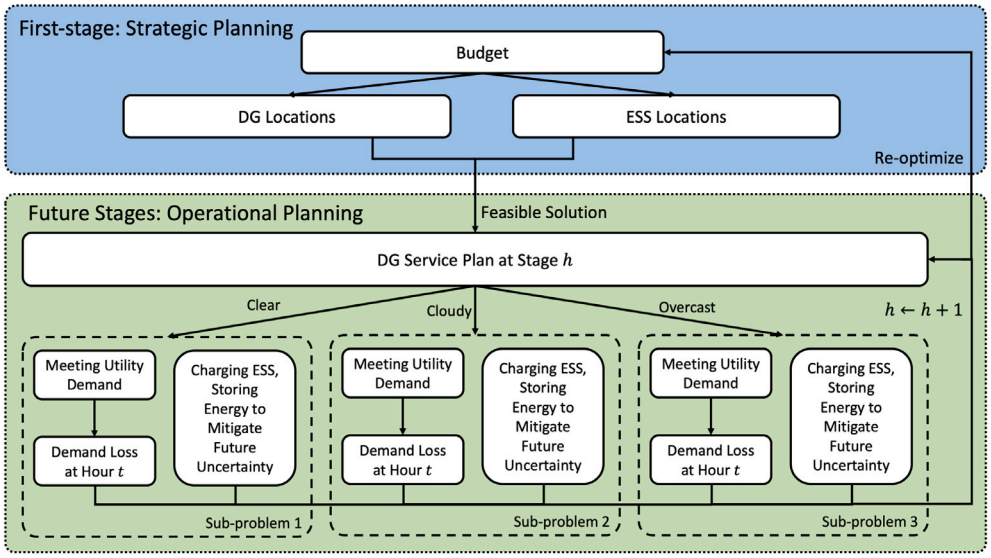

Fig. 1. An illustrative pipeline of the proposed multi-stage stochastic optimization model. The first stage decides the optimal numbers and locations of DGs and ESSs within the microgrid from a strategic planning perspective. The future stages, with the consideration of operational planning, meet the demands of the critical loads by incorporating optimal power supply plans and ESS charging/discharging options. Solutions from future stages are propagated back to the first stage iteratively to achieve an exact optimal solution.

due to the ability to locate distributed generators (DGs) closer to the power consumer and the use of renewables helps reduce the carbon footprint of power generation as well [11,12].

1.2. Research motivation

The rise in disaster-caused power outages has pushed the US government to implement federal policies that request the development of operational, technical, and economic models, which depict the disaster-relief power supply benefits that microgrids can provide utilities [13,14]. In such situations, utilities typically face the brunt of public criticism and pressure to get the damaged main grid back to normal functionality. In the case of critical loads within a utility's serviced region, utility-owned microgrids can reliably provide uninterrupted disaster relief power supply to the buildings, thus ensuring that the public maintains access to the resources the critical loads provide. There are growing concerns that the frequency and length of power outages caused by weather-related disruptions to the power grid will increase in the coming years due to climate change patterns [9,15]. The development of models that capture microgrid reliability over long-term power outage durations can help build a case for utilities to move towards a larger scale of microgrid adoption than is presently witnessed [16].

Thus, in order to optimize microgrid reliability during long-term power outages, we propose a multi-stage stochastic program that models the techno-economics of microgrid investment, operation and maintenance, reliability and resilience for an islanded utility-scale microgrid, over a week-long power outage duration. The model is developed from a utility perspective and includes budget limitations for the microgrid investment costs. We use solar (photovoltaic — PV) DGs, which are easier to install in rural and urban areas through rooftop mounting. Our model focuses on the daytime period (6 am–6 pm), when PV generation is possible, and assumes that the backup generators possessed by each critical building provide the nighttime power.

Specifically, the model considers the uncertainty of daily DG power output based on the hour and weather (cloud coverage) of each day, and provides a holistic objective function that captures the investment, fixed operation and maintenance, power supply efficiency, reliability and resilience of the microgrid in terms of a minimized total cost for the utility. This is accomplished through the optimization of the size, location, power supply assignment, and the total number of DGs and ESSs within a utility-owned microgrid. Fig. 1 depicts a pipeline of the proposed modeling approach. In the first-stage, the model decides the optimal numbers and locations of DGs and ESSs within the microgrid, where the total investment cost is subject to a utility budget constraint. Then, during the future stages, the operational planning of the microgrid is optimized using multiple sub-problems to meet the demands of the critical loads. Sub-problems at stage (day) h are constructed under different weather scenarios, and are strongly linked with those at stage $h+1$, since the charging/discharging operations of ESSs directly affect the amount of power available for future operations. Solutions from the future stages are propagated back to the first stage as the decisions must be made in the first stage

Considering the large scale of the multi-stage stochastic model, a sophisticated solution algorithm is used, which analyzes the microgrid's reliability across all possible weather scenarios (e.g., clear, cloudy, overcast) of a week-long outage (3279 total scenarios). The model is also applied to a case study that contains a developed network of 5 and 10 critical load nodes. The Euclidean distance between the nodes serves as the distance power travels for supply in this research. The model proposed in this research extends a previously developed stochastic model that did not include energy storage systems [17].

2. Literature review

We perform a review of past literature where the following is highlighted: (1) utility-partnered microgrid construction for reliable power supply post-disasters from the past decade; (2) optimization modeling of islanded microgrids for reliable power supply of critical loads post-disaster; and (3) recent modeling techniques for optimizing islanded microgrid reliability.

2.1. Utility-partnered microgrid construction for power supply after natural disaster

Over the last decade, it has become clear that maintaining public health and safety during a natural disaster requires the efficient and effective operation of critical loads and services, including energy, food and water, communications, shelter, emergency response, and transportation. Locations that prove to be vulnerable to major grid disturbances, due to natural disasters, are turning to microgrids to help mend similar issues [18]. As a result, there has been a surge

in microgrid development that is utility-partnered to provide reliable power supply in the aftermath of disaster caused outages [19]. In 2011, residents in Sendai, Japan went without power for three days as a result of a 9.0 magnitude earthquake and tsunami. Because the natural disasters severely impacted the main grid, utility power was interrupted for 60% of Sendai's loads. The Sendai microgrid, created in tandem with a utility, provided power to the Tohuku Fukushi University Teaching Hospital after the disaster caused outage [20]. Another utility-partnered microgrid development for reliable post-disaster power supply is located at the Public Safety Headquarters (PSHQ) in Montgomery County, Maryland. The microgrid was constructed as a way to secure the vital public services held at the PSHQ, including the Emergency Management and Homeland Security offices, in addition to the police station serving a large segment of the county [21]. A surge in wildfires and earthquakes caused a formation of a microgrid composed of three-fire stations in Fremont, California after fire stations found challenges with backup generators that only lasted 72 h before being renewed. Because these PV-DGs were added to the location of these fire stations, thus helping to form the microgrid, they furthered the available amount of hours for disaster power supply and lessened the vulnerability of the fire stations during power outages. This type of microgrid highlighted the importance of providing critical loads with the ability to island from the grid, and was essentially the debut of a US microgrid where DGs are constructed directly at the critical load [22].

2.2. Optimizing islanded microgrids for critical load power restoration post-disaster outages

From the research perspective, modeling approaches have been proposed to optimize islanded microgrids for power restoration of critical loads during disaster-caused power outages. Some of these approaches implement multi-objective optimization with objectives for minimizing microgrid costs and maximizing the generation capacity of the microgrid [23], while others aim to maximize critical loads restored (microgrid reliability) and minimize total microgrid costs [10]. Some focus on single-objective optimization and aim to minimize the distance of population centers to critical loads by optimizing DG location within the microgrid [11], while others only aim to maximize the total power of restored loads [24]. An in-depth review was recently conducted in the literature to investigate energy management optimization approaches for islanded microgrids [25]. The authors state that commonly-used objectives in islanded microgrid optimization aim to optimize power generation capacity of the microgrid (maximization), power loses from unused or excess power (minimization), total microgrid system costs — installation, location, operation and maintenance costs of DGs and ESSs in the microgrid (minimization), and expected load/demand met or restored (maximization) - also known as the microgrid's reliability. Research investigating the mentioned objectives as combined in one holistic objective, which coordinates techno-economic analysis and system performance of islanded microgrids, has not been well studied [26]. The proposed model in this research combines these commonly-used islanded microgrid optimization objectives into a holistic objective function that not only accounts for the total costs, power generation capacity, and potential power losses of the microgrid, but also captures the reliability and resilience of the microgrid, as one minimized total cost objective for the utility.

2.3. Optimizing islanded microgrid reliability

Microgrids offer clean and secure sources of power even in the most remote, unstable locations. However, an uninterrupted supply of power is essential. Therefore, the reliability of a microgrid, especially when islanded, is an important aspect. Microgrid system reliability is a metric that assesses a microgrid's overall ability to adequately generate and distribute uninterrupted power to expected loads. Different techniques are used to measure the reliability of a microgrid that include CAIFI (customer average interruption frequency index), SAIDI (system average interruption duration index), SAIFI (system average interruption frequency index), EENS (expected energy not supplied), and the LOLE (loss of load expectation) [27–30]. Reliability analysis that combines SAIFI, SAIDI and CAIFI and captures both reliability and supply-adequacy concerns of an islanded microgrid is discussed in [31]. Reliability evaluation indexes have also been converted to costs and minimized in other work. For example, researchers in [32] optimize the reliability of an islanded microgrid by determining the optimal capacities of ESSs to minimize a cost-based version of EENS. A version of LOLE is used to measure islanded microgrid reliability in [33], where ESS sizing is optimized in a manner where the net profit of the microgrid is maximized. Wu and Sansavini [34] optimize the capacities and placements of distributed energy resources within an islanded microgrid, and model EENS as a reliability cost that is minimized in the objective.

In the literature, the impact of the stochastic environment on microgrid reliability has been widely considered, with applications to power-water distribution systems [35], or with battery swapping stations [36]. In many studies, two-stage stochastic programs are formulated to model the stochastic effects under different scenarios. However, most studies optimize islanded microgrid reliability over short-term to medium-term (hours to days) power outage durations [25,35]. To the best of our knowledge, optimization approaches for islanded microgrid reliability over long-term outage horizons, with the effects of uncertain daily weather (cloud coverage) on daily PV output considered, have not been well studied. In addition, few have studied the techno-economics and operations of an islanded microgrid combined with ESSs. The proposed model bridges the gap by optimizing the islanded DG+ESS microgrid dependability over a long-term outage (week-long), adopting a variant of the EENS reliability technique.

2.4. Main contributions

This research models the techno-economics of microgrid investment, operation and maintenance, reliability, and resilience for an islanded utility-owned microgrid over the course of a week-long power outage by optimizing the location, sizing, power supply assignment, and the total number of DGs and ESSs within the microgrid. The following are the major contributions of this research. First, we propose a multi-stage stochastic program to optimize the reliability of a DG+ESS microgrid under stochastic weather conditions in the long term. The model captures essential elements in microgrid operations, such as the initial investment budget, operation and maintenance cost, power supply efficiency, reliability and resilience. Second, we implement a sophisticated solution algorithm, namely the nested L-shaped algorithm, as an exact solution approach to the multi-stage model. Specifically, the algorithm optimizes daily DG power output and ESS charge/discharge over a week-long (7 days) period, with uncertainties in each day's weather (thus 3279 day–weather scenarios in total). Third, we conduct numerical studies using data from the real world to validate the proposed model. We gather data from a middle-sized city in the U.S., and consider up to 10 critical facilities across the city. Results are summarized, and insights are drawn from model outputs.

3. Model formulation

The model formulation is described in this section. The formulation combines the multi-source facility location problem described in [37] and the location coverage problem described in [38] and [39], as well as the assumptions. We refer to the problem as a multi-source capacitated facility location coverage problem (MS-CFLCP) due to the multiple sources for power supply/demand coverage within the microgrid, all of which have a limited capacity. The MS-CFLCP is formulated as a multi-stage stochastic program because the storage systems contain memory from stage to stage (day to day), and is solved using nested

Table 1
Nomenclature.

Index	Description
Sets	
i	Building nodes with power demand $\{1, 2, \ldots, n\}$, where $n = 5, 10$
j	Building nodes that are candidate PV-DG locations $\{1, 2, \ldots, m\}$, where $m = 5, 10$
w	Cloud coverage (weather) conditions (clear, cloudy and overcast) $\{1, 2, 3\}$
h	Stages $\{1, 2, \ldots, H\}$, where each stage 2–8 represents a different day of the week-long outage
Variables	
	$D_j = \begin{cases} 1 & \text{if PV-DG is located at building/node } j \\ 0 & \text{otherwise} \end{cases}$
	$S_j = \begin{cases} 1 & \text{if an ESS is located at building/node } j \\ 0 & \text{otherwise} \end{cases}$
	$x_{i,j}^{h,w} =$ power amount supplied from PV-DG located at j to building/demand node i during stage h with weather condition (cloud coverage) w, where $x_{i,j}^{h,w} \geq 0$ in W
	$y_{i,j}^{h,w} =$ stored power amount supplied from ESS j to building/demand node i during stage h with weather condition (cloud coverage) w, where $y_{i,j}^{h,w} \geq 0$ in W
	$l_i^{h,w} =$ amount of unmet demand for building/demand node i during stage h with weather condition (cloud coverage) w, where $l_i^{h,w} \geq 0$ in W
	$\gamma_i^{h,w} =$ amount of excess power at building/demand node i during stage h with weather condition (cloud coverage) w, where $\gamma_i^{h,w} \geq 0$ in W
	$\omega_j^{h,w} =$ amount of stored power in ESS j at the end stage h with weather condition (cloud coverage) w, where $\omega_j^{h,w} \geq 0$ in W
	$\epsilon_j^{h,w} =$ amount of power charged to ESS j during stage h with weather condition (cloud coverage) w, where $\epsilon_j^{h,w} \geq 0$ in W
PV-DG Parameters	
a	Minimum total of PV-DGs within the microgrid
B	Utility budget for microgrid investment
ϑ	Rate of power losses
$\delta_i^{h,w}$	Demand of power at node i during stage h with weather w (cloud coverage) in W
α_j	Size of PV-DG j in W
$o_j^{h,w}$	Output power from PV-DG at j during stage h with weather w (cloud coverage) in W
ϕ_j	Operation and maintenance (O&M) costs for PV-DG at j in \$/W
λ_j	Penalty applied for excess PV-DG and ESS power at j in \$/W
ψ_i	Penalty applied for not meeting the demand of power at node i in \$/W; penalty is applied based on the importance of node
I_j	Cost to invest in a utility-scale PV-DG at node j in \$/W
d_{ij}	Matrix $(n \times m)$ of distances between each location of demand node i and PV-DG j; distances represent cost to distribute power across each distance
Storage Parameters	
η_j	Size of ESS j in W
ζ_j	Investment cost of a utility-scale ESS j in \$/W; investment cost includes the capital costs for energy capacity, power conversion system costs, balance of plant costs, interconnecting transformers, construction and commissioning costs
μ_j	Operation and maintenance O&M costs for ESS j in \$/W
β_j	Initial stored power in ESS j in W
Ω_j	Capacity of an ESS j in W
e_d	Discharge efficiency of an ESS; assumed as 99%
e_c	Charge efficiency of an ESS; assumed as 99%

Benders decomposition (also known as nested L-shaped method for multi-stage models). The model's nomenclature is provided in Table 1.

The model considers the microgrid's reliability performance to meet customer demands over every possible one of the 3279 scenarios. The resilience of the microgrid is captured by minimizing the potential reverse power flow in the system. Since we are modeling an islanded microgrid, any excess power at a building will reverse its flow due to the microgrid being disconnected from the main grid. Reverse power flow, which is caused by excess renewable generation, has system functionality consequences such as voltage peaks and reduced power quality [40]. Such issues, especially when considering utility-scale generation as we do in this research, can make the microgrid less resilient to a system failure. Thus, the model aims to minimize the reverse power flow within the network. The model is designed from a utility perspective and includes budget considerations for the microgrid investment costs. The solutions portray the total costs and reliability of various islanded microgrid configurations based on allocated utility budget options.

3.1. First-stage

Let $h = 1, 2, \ldots, H$ denote the stages of the MS-CFLCP, where $H \in \mathbb{N}^+$ is the maximum horizon. Each stage h represents one day of the week-long outage and contains 12 daytime hours of power demand for each building aggregated. PV-DGs and ESSs can be installed at location $j \in M := \{1, 2, \ldots, m\}$ to satisfy the demand at locations $i \in N := \{1, \ldots, n\}$; each building serves as a candidate to locate a PV-DG and or ESS. We analyze a 5-building network where M and N both equal 5, as well as a 10-building network where M and N both equal 10. Note that the model allows $M \neq N$. Using different M and N only affects the power balance equations, which will be introduced in Eqs. (12) and (13) in later sections, since the power balance equation for a location in M is different from that of a location in N. To account for the weather (cloud coverage) uncertainty in PV-DG power output, let $w = 1, 2, 3$ denote the weather (cloud coverage) condition of each day, where $w = 1$ represents a clear day with a large output of PV-DG power, $w = 2$ represents a cloudy day with low power output from PV-DGs and $w = 3$ represents a day with overcast skies and extremely low

PV-DG power output. In the first-stage program, decisions are made for the location PV-DGs and ESSs as described below:

$$\min \quad \sum_{j\in M}\left(I_j\alpha_j D_j+\zeta_j\eta_j S_j\right)+\sum_{j\in M}\left(\phi_j\alpha_j D_j+\mu_j\eta_j S_j\right)+\mathcal{Q}^2(\boldsymbol{D},\boldsymbol{S},\boldsymbol{\omega^1}) \tag{1}$$

$$\text{s.t.} \quad \sum_{j\in M} D_j \geq a; \tag{2}$$

$$\sum_{j\in M}\left(I_j\alpha_j D_j+\zeta_j\mu_j S_j\right)\leq B; \tag{3}$$

$$\omega_j^1=\beta_j S_j \quad \forall j\in M; \tag{4}$$

$$D_j, S_j\in\{0,1\} \quad \forall j\in M. \tag{5}$$

The objective function is described in Eq. (1) and is a minimization of the total cost for locating (investment cost) PV-DGs ($D_j s$) and ESSs ($S_j s$), plus the total fixed O&M costs for PV-DGs and ESSs; we formulate the two cost functions separately since we provide each cost separately in the results. $\mathcal{Q}^2(\boldsymbol{D},\boldsymbol{S},\boldsymbol{\omega^1})$ denotes the expected objective value of the sub-problem stages. Eq. (2) ensures that a minimum of a PV-DGs are located in the microgrid; we analyze two versions of the MS-CFLCP where we assume that $a\geq 0$ in one model and $a\geq 1$ in the second. We include Eq. (2) for model flexibility if a utility were to desire a certain minimum number of PV-DGs be located; this would be advantageous for a utility servicing a region with a large percentage of clear weather (cloud coverage) versus a utility in a region with predominantly cloudy and overcast weather. Eq. (3) ensures the total cost to install/locate (investment cost) PV-DGs and ESSs is within a pre-determined utility budget B. Eq. (4) ensures that an installed ESS (S_j) at location j has initial power β_j available to use at the beginning; we assume ESSs begin the week-long outage with 100% initial power due to them charging in the time leading up to the main grid disturbance caused by the natural disaster. Eq. (5) ensures that PV-DG and ESS decision variables D_j and S_j, respectively, are binary.

3.2. Sub-problem stages

In Eq. (1), $\mathcal{Q}^2(\boldsymbol{D},\boldsymbol{S},\boldsymbol{\omega^1})$ is the aggregated objective of the sub-problem stages, where in each stage, the model decides how much power is supplied from a located PV-DG and or an ESS j to a building at demand node i during stage h with weather condition w (cloud coverage) . At stage $h-1$, where $h\geq 2$, we have

$$\mathcal{Q}^h(\boldsymbol{D},\boldsymbol{S},\boldsymbol{\omega^{h-1}}):=\mathbb{E}_{(w)}[\mathcal{Q}^h(\boldsymbol{D},\boldsymbol{S},\boldsymbol{\omega^{h-1}},w)], \tag{6}$$

as the expected objective value of stage h, where $\mathbb{E}_{(w)}$ represents the expectation for the weather (cloud coverage) parameter and

$$\begin{aligned}\mathcal{Q}^h(\boldsymbol{D},\boldsymbol{S},\boldsymbol{\omega^{h-1}},w):=\min \quad & z=(1-\vartheta)\sum_{i\in N}\sum_{j\in M} d_{i,j}(x_{i,j}^{h,w}+y_{i,j}^{h,w})\\ &+\sum_{i\in N}\psi_i l_i^{h,w}+\sum_{i\in N}\lambda_i\gamma_i^{h,w}\\ &+\mathcal{Q}^{h+1}(\boldsymbol{D},\boldsymbol{S},\boldsymbol{\omega^h}).\end{aligned} \tag{7}$$

The first term of z, $d_{i,j}(x_{i,j}^{h,w}+y_{i,j}^{h,w})$, computes the total cost of the power supply based on the distance traveled to supply the power where $(1-\vartheta)$ estimates the power losses witnessed during power delivery from PV-DGs and ESSs to critical loads. Since more power is lost in distribution and the further DGs and ESSs are from the demand sites, this cost function aims to minimize the distance between a demand site and its supplying DG and or ESS. It in-turn would reduce the potential losses as power is transmitted and improves the power supply efficiency of the microgrid. We are modeling the microgrid network as a facility location problem network due to the use of comprehensive DG and ESS investment costs from the model's first-stage, which account for the entirety of the microgrid's development. Thus in the sub-problem states, the Euclidean distance between a DG and or ESS and a building demand node ($d_{i,j}$) is used as a supply cost (similar to the links in a facility location problem) that represents the distance traveled for power distribution [41]. The second item of z computes the cost of unmet demand, where $l_i^{h,w}$ is the amount of unmet demand and ψ_i is the unmet demand penalty coefficient. The third item computes the cost of excess power, where $\gamma_i^{h,w}$ is the amount of excess power penetrated and λ_i is the excess power penalty coefficient. The last term of z, $\mathcal{Q}^{h+1}(\boldsymbol{D},\boldsymbol{S},\boldsymbol{\omega^h})$ denotes the aggregated objective of the proceeding stages of the model. The sub-problems at each stage h are subject to the following constraints:

$$\text{s.t.} \quad \sum_{i\in N} x_{i,j}^{h,w}\leq o_j^{h,w}D_j \quad \forall\, j\in M; \tag{8}$$

$$\sum_{i\in N} y_{i,j}^{h,w}\leq e_d\ \omega_j^{h-1} \quad \forall\, j\in M; \tag{9}$$

$$\omega_j^{h,w}=\omega_j^{h-1}-\frac{1}{e_d}\sum_{i\in N} y_{i,j}^{h,w}+e_c\ \epsilon_j^{h,w} \quad \forall\, j\in M; \tag{10}$$

$$\omega_j^{h,w}\leq \Omega_j\ S_j \quad \forall\, j\in M; \tag{11}$$

$$\begin{aligned}&o_i^{h,w}D_i+\sum_{j\in M, j\neq i} x_{i,j}^{h,w}+\sum_{j\in M} y_{i,j}^{h,w}\\ &\quad=\sum_{j\in N, j\neq i} x_{j,i}^{h,w}+(\delta_i^{h,w}-l_i^{h,w})+\epsilon_i^{h,w}+\gamma_i^{h,w} \quad \forall\, i\in N\cup M;\end{aligned} \tag{12}$$

$$\sum_{j\in M, j\neq i} x_{i,j}^{h,w}+\sum_{j\in M} y_{i,j}^{h,w}=(\delta_i^{h,w}-l_i^{h,w})+\gamma_i^{h,w} \quad \forall\, i\in N\setminus M; \tag{13}$$

$$l_i^{h,w}\geq \delta_i^{h,w}-\sum_{j\in M}(x_{i,j}^{w,h}+y_{i,j}^{h,w}) \quad \forall\, i\in N \tag{14}$$

$$l_i^{h,w}\leq \delta_i^{h,w} \quad \forall\, i\in N \tag{15}$$

$$x_{i,j}^{h,w}, y_{i,j}^{h,w}\geq 0 \quad \forall\, i\in N, j\in M; \tag{16}$$

$$l_i^{h,w}, \gamma_i^{h,w}\geq 0 \quad \forall\, i\in N; \tag{17}$$

$$\omega_j^{h,w}, \epsilon_j^{h,w}\geq 0 \quad \forall\, j\in M. \tag{18}$$

Eq. (8) ensures the power amount supplied from PV-DG j to it is assigned critical loads i during stage h with weather condition (cloud coverage) w ($x_{i,j}^{h,w}$) is within the power output from the PV-DG j during stage h with weather condition (cloud coverage) w ($o_j^{h,w}$); this is for all PV-DGs. Eq. (9) ensures that the amount of power supplied by an ESS at location j is less than the power stored in the ESS at the end of stage $h-1$. In the constraint, e_d is the discharge efficiency of an ESS. Eq. (10) is the ESS power flow balance constraint. It ensures that the presently stored power at stage h under weather (cloud coverage) condition w ($\omega_j^{h,w}$) of each ESS j must equal to the stored power available at the end of stage $h-1$ minus the stored power usage in stage h, plus the power charged into the ESS at stage h; e_c is the charge efficiency of an ESS. Eq. (11) ensures that the presently stored power at stage h under weather (cloud coverage) condition w ($\omega_j^{h,w}$) of an ESS j is limited by the storage capacity (Ω_j) of that ESS j.

Eqs. (12) and (13) ensure the power flow balance at each node/site i. For each demand node/critical load i that is also a potential site for the location of a PV-DG and or ESS j, the left-hand-side of Eq. (12) represents the power available at a site i: the power output at site i if a PV-DG is installed ($o_i^{h,w}D_i$) and the sum of all power supplied to site i from PV-DGs and ESSs at other locations ($x_{i,j}^{h,w}+y_{i,j}^{h,w}$). The right-hand-side of Eq. (12) represents the power usage at site i: the power supplied to other sites from the installed PV-DG j at site i ($x_{j,i}^{h,w}$, where $j\neq i$), the power used to satisfy the demand of the critical load at site i ($\delta_i^{h,w}-l_i^{h,w}$), the power used to charge the ESS at site i ($\epsilon_i^{h,w}$), and the excess power at site i ($\gamma_i^{h,w}$). For each demand node/critical load site i where PV-DGs and ESSs are not installed, the left-hand-side of Eq. (13) represents the sum of all power supplied to site i from PV-DGs and ESSs at other locations ($x_{i,j}^{h,w}+y_{i,j}^{h,w}$). The right-hand-side of Eq. (13) represents the power usage at site i: the power used to satisfy the demand of the critical load at site i ($\delta_i^{h,w}-l_i^{h,w}$) and the excess power at site i ($\gamma_i^{h,w}$). For both Eqs. (12) and (13), the demand of the critical load ($\delta_i^{h,w}$) minus the unmet demand of the building ($l_i^{h,w}$) equates to the demand met or satisfied for the building.

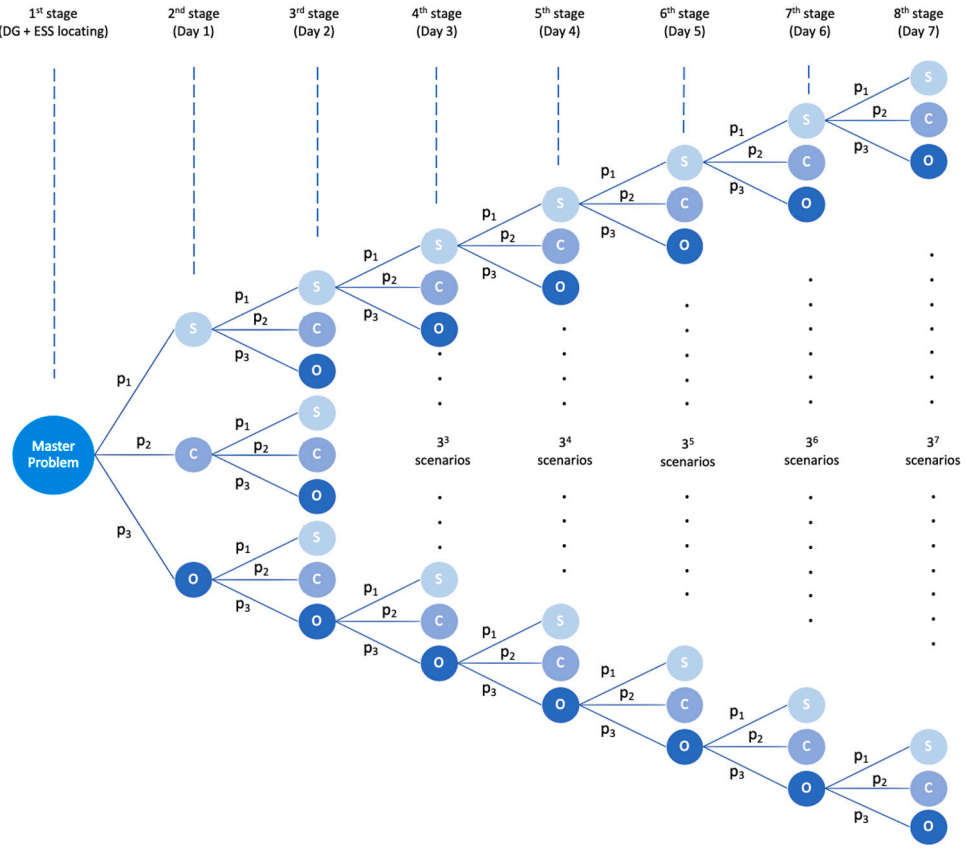

Fig. 2. MS-CFLCP model node-scenario tree diagram, where p_1 = 27%, p_2 = 29% and p_3 = 44% represent the probability of the day experiencing clear or sunny (S), cloudy (C) and overcast (O) weather (cloud coverage) respectively. The model has a total of 3279 scenarios of day–weather (day and weather combination) over the duration of a week-long outage.

Eq. (14) ensures that the minimum amount of unmet demand at site i is bound by the difference of the demand at stage h under weather (cloud coverage) w ($\delta_i^{h,w}$) and the aggregated amount of power supplied to i from other locations ($x_{i,j}^{h,w} + y_{i,j}^{h,w}$). Note that together with Eq. (12), the model has the freedom to "sacrifice" part of the demand at a location $i \in N \cup M$, so that more power can be stored into the ESS to meet future demands. In that case, Eq. (14) will not be binding. Eq. (15) ensures that the unmet demand at a location i ($l_i^{h,w}$) cannot exceed the total demand of i ($\delta_i^{h,w}$). Eqs. (16), (17) and (18) ensure that the PV-DG power supply ($x_{i,j}^{h,w}$), ESS power supply ($y_{i,j}^{h,w}$), unmet power demand ($l_i^{h,w}$), excess power ($\gamma_i^{h,w}$), presently stored power ($\omega_j^{h,w}$) and power charged to an ESS ($\epsilon_j^{h,w}$) variables are continuous.

Fig. 2 displays the scenario tree diagram for the MS-CFLCP with all stages of the multi-stage model portrayed, as well as the number of scenarios in each stage. Each combination of day-and-weather ($h - w$) represents a different scenario. The best-case full week-long scenario would be a week where all 7 days experience clear weather (no cloud coverage), while the worst-case would be a week where all 7 days experience overcast weather (cloud coverage).

3.3. Assumptions

The following assumption are used in the modeling of the MS-CFLCP : (1) the maximum number of PV-DGs and ESSs that can be located is known and is based on the number of candidate locations available; (2) candidate locations for PV-DG and ESS exist within an operational microgrid system that is fully interconnected due to the comprehensive DG and ESS investment costs from the model's first-stage, which accounts for the entirety of the microgrid's development (DG investment includes the modules and inverter costs, costs for balance of system components (structural and electrical), labor costs for installation, transmission lines and interconnection, taxes and overhead, inspection and permitting, and land acquisition; ESS investment cost includes the capital costs for energy capacity, power conversion system costs, balance of plant costs, interconnecting transformers, construction and commissioning costs); (3) the full year has an estimated 97, 107, and 161 days of clear, cloudy, and overcast weather respectively in the case study [42]; (4) the microgrid is in island mode operation after a major disturbance on the main grid, where all power supplied comes from the located DGs and or ESSs; (5) ESSs begin the outage week at full charge with the assumption that utility managers would have enough time to charge the ESSs based on updates from local news cycles tracking a natural disaster's arrival in the utility's serviced region; and (6) the microgrid supplies power throughout the daytime period (6 am–6 pm), while the backup generators each critical load is assumed to possess supply power when the sun is no longer available. Python programming language and GUROBI optimizer were used to solve the model on a Tesla GPU server.

4. Solution methodology

The nested L-shaped algorithm is a decomposition method applied to multi-stage stochastic problems. The algorithm decomposes the master problem being solved into smaller sub-problems that can be solved independently. The solutions to the decomposed sub-problems are reintegrated back into the master problem to solve the overall problem. Depicting the algorithm is primarily accomplished with the use of a node-scenario tree diagram, where each node on the tree represents

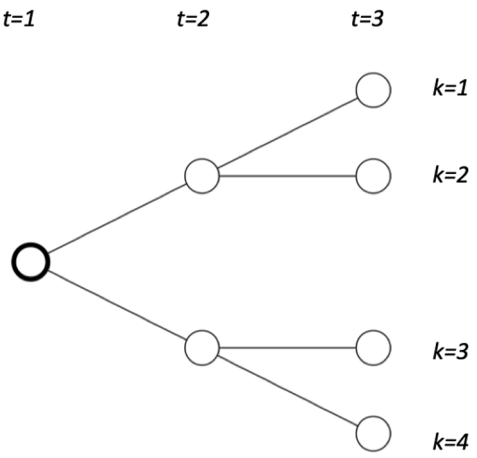

Fig. 3. An example of a node-scenario tree diagram. Each branch has a certain probability of occurring..

a specific decision period and the number of nodes in each period represents the number of possible scenarios at that period; the number of nodes in the last period of the node-scenario tree diagram is equivalent to the total possible outcomes of the master problem [43]. Fig. 3 displays an example of multi-stage node-scenario tree, where t represents the period (stage) and thus there are 3 stages portrayed in Fig. 3. Period $t = 1$ represents the root node, which is the overall master problem. Each node following the root node is a leaf node of the tree diagram. Each leaf node within a specific period t represents a possible scenario outcome of the period t. The four-leaf nodes in period $t = 3$ ($k = 1, \dots, 4$) represent the scenarios in period $t = 3$. Since period $t = 3$ is the last period (stage), it means that there are four total outcomes for the problem.

At each decision period (sub-problem), an optimization problem is solved. Once sub-problem solutions are reintegrated back into the root node, an optimal decision or optimal solution can be determined for the master problem. The decision or solution at each node affects the problem being solved at the consecutive node; this is referred to as a recourse problem, where an initial decision is made at one time period, time passes during which events occur, and then a new decision (recourse decision) is made that optimizes the solution taking into account the events that have occurred since the previous decision's time period [43].

4.1. Nested decomposition

The general nested L-shaped problem has a set of stages $t = 1, \dots, H-1$ and a set of scenarios $k = 1, \dots, \mathscr{K}^t$, where H is the total number of stages and $\mathscr{K}^t$ is the number of distinct scenarios at stage t. Cuts, to stage $t-1$ and solutions for stage $t+1$ are generated from the following master problem [44]:

$$\min \quad (c_k^t)^T x_k^t + \theta_k^t \tag{19}$$

$$\text{s.t.} \quad W^t x_k^t = h_k^t - T_k^{t-1} x_{a(k)}^{t-1}; \tag{20}$$

$$D_{k,j}^t x_k^t \geq d_{k,j}^t; \qquad \forall j = 1, \dots, r_k^t; \tag{21}$$

$$E_{k,j}^t x_k^t + \theta_k^t \geq e_{k,j}^t; \qquad \forall j = 1, \dots, s_k^t; \tag{22}$$

$$x_k^t \geq 0. \tag{23}$$

In the above master problem $a(k)$ represents the ancestor scenario of k at stage $t-1$. $x_{a(k)}^{t-1}$ represents the current solution from $a(k)$. The problem has boundary conditions at the first-stage, $t = 1$, and last stage. The initial conditions for $t = 1$, the first-stage, are $b = h^1 - T^0 x^0$. For stage H, the last stage, θ_k^H, constraint (21) and (22) are removed. Each sub-problem is called a Nested L-shaped decomposition sub-problem and is denoted as $NLDS(t, k)$. The following section details the implementation of the nested L-shaped method.

4.2. Implementation of nested L-shaped method in MS-CFLCP

Applying the nested L-shaped method requires knowledge of how to move forward and backward on the tree nodes. This begins by solving the root node in the *first-stage* without consideration of any constraints from its subsequent nodes (sub-problems). The optimal solution to the root node is then used to solve the proceeding leaf nodes of the root node (sub-problems); this is the *second-stage* and feasibility and optimality cuts for the first-stage are generated at this step.

Feasibility cuts are constraints generated and added to the first-stage problem when a sub-problem is determined infeasible based on the solution of the first-stage. Generally, feasibility cuts will help make a previously infeasible sub-problem feasible and thus provide a feasible solution to the master problem. Note that feasibility cuts cannot guarantee an optimal master problem solution. In the MS-CFLCP, however, feasibility cuts are unnecessary since every sub-problem in stages $h = 2, 3, \dots$ has complete recourse, i.e., for any solution $(\boldsymbol{D}, \boldsymbol{S}, \boldsymbol{w}^{h-1})$, the sub-problem in stage h is always feasible. The feasibility of sub-problems is primarily ensured by the model setup. In island mode, when access to the main power grid is cut off, it would be too ambitious to assume that the microgrid can support all the demand from critical loads. The best course of action is to reduce the unmet demand (demand loss) as much as possible, considering the importance of the loads. Thus, in the model, power demands are modeled as costs in the objective, rather than constraints that have to be satisfied, guaranteeing feasibility in every sub-problems.

As such, in the MS-CFLCP, only optimality cuts are generated. Optimality cuts send information back to the first-stage problem about how to make the first-stage solution an optimal one and not just a feasible solution [43]. Typically, optimality cuts are derived from the dual variables of a sub-problem. Due to the complexity of the sub-problems, we are unable to formulate the dual problem of the MS-CFLCP explicitly. However, thanks to modern commercial solvers such as GUROBI, information about the dual variables is directly accessible after solving the primal sub-problems of the MS-CFLCP so that optimality cuts can be derived without formulating the dual problem in its closed form.

After solving the second-stage, we have two options: (1) go backwards to the root node problem using the cuts generated from the second-stage problems; (2) use the optimal solutions determined for the second-stage problems and move forwards to the *third-stage* to solve the sub-problems of the third-stage without consideration of any constraints in subsequent nodes (sub-problems); solving the third-stage sub-problems generates cuts for the second-stage problems. The process continues, with solutions passed down the tree from parent nodes to children nodes while cuts are passed back up the tree from children nodes to parent nodes, until the bottom nodes of the tree are reached and the algorithm can only move back up the tree. The algorithm cannot move further down any tree branch where infeasibility has occurred at a node (sub-problem) because there would be no proposed solution to pass to the children nodes from the parent node. The following subsection details the sequencing protocols used to help decide which way the algorithm moves (forward/down or backwards/up) and when, as well as when to terminate the algorithm's movement through the tree [43].

4.3. Sequencing protocols

The three main sequencing protocols are *fast-forward, fast-back*, and *fast-forward-fast-back*. *Fast-forward* moves forward/down the tree, and movement forward/down is dictated by the finding of a feasible solution at the present sub-problem/node. Each determined feasible

solution at the sub-problem is taken to the children nodes of that sub-problem until the leaves at the end of the tree are reached, or an infeasible sub-problem node is reached. *Fast-back* moves backward/up the tree. When an optimality cut is added at a child node, the algorithm moves backward to re-solve the parent node. This process repeats until the root node (first-stage problem) is reached and re-solved for an optimal solution. *Fast-forward-fast-back* combines the fast-forward and fast-back sequencing protocols. The algorithm moves forward/down the tree until it can go no further and then switches to moving backward/up the tree until the root node.

The algorithm concludes at termination. *Termination* is reached when all sub-problems at all stages of the tree are feasible based on the first-stage solution. While navigating through the tree, the algorithm will terminate and find the entire problem infeasible if the root node/first-stage solution becomes infeasible. If all sub-problems are feasible with the current first-stage solution, and all sub-problems have reached an optimal solution, the algorithm will terminate.

5. Tennessee case study

A case study is used to analyze the performance of the model. The case study contains critical loads from an area in Tennessee, where each building doubles as one of the candidate location sites for a PV-DG and or ESS. The model uses three PV-DG system sizes of 500 kW, 1 MW, and 5 MW. All ESSs are 1 MW in size. Benchmark cost reports by NREL state that PV-DG rooftop mounting is possible for 3 kW–2 MW sized PV-DGs, while ground mounting is used for PV-DGs of sizes greater than 2 MW; such large PV-DGs require land acquisition [45]. For this study, hospitals and large-scale grocery stores serve as candidates for the location of 5 MW PV-DG systems, police and fire stations serve as candidates for the location of 1 MW PV-DG systems, while gas stations serve as candidates for the location of 500 kW PV-DG systems. We describe the PV-DG power output data and the uncertainty experienced within power output, the cost data for the PV-DGs and ESSs, the critical loads power demand data and the uncertainty within the demand, the penalty for unmet demand at each building type, as well as the 5-building and 10-building networks we use for modeling in this section. The data used in this model is also available for viewing and downloading in a table format at Kizito [46].

5.1. PV-DG power output

Weather effects (i.e., cloud coverage) in addition to the time-of-day trigger natural uncertainty in PV-DG power output. In this study, we consider three weather conditions, namely, clear, cloudy and overcast, as defined according to the National Center for Environmental Information (NCEI) [47]. Each weather condition represents an independent scenario in each stage of sub-problems. The weather conditions follow a discrete probability distribution, estimated based on the data provided by the NCEI, with clear, cloudy and overcast corresponding to probabilities $[0.27, 0.29, 0.44]$, respectively [47].

We use NREL's PVWatts calculator to provide estimated power outputs, using annual and hourly averages for each PV-DG system. Power output is determined for daytime hour using the PV irradiance (W/m^2) and is provided for each day of the year by NREL's PVWatts [48]. PV irradiance from day 15 of each month is used to determine the percentage of the total irradiance witnessed for each daytime hour. This is done due to daylight savings, which causes the increases in irradiance during the morning hours (i.e., 6 am–7 am) and later in the afternoon (i.e., 5 pm–6 pm) when the days are longer. The irradiance percentage at each daytime hour is then multiplied by the power output for each type of PV-DG. This provides an estimate for the output power at each daytime hour. We then aggregate these 12 h of power output, thus giving us a daily estimate of power output for each PV-DG type.

The PV-DG power outputs, determined by PVWatts, are set as the estimates for a "clear day" to help account for the weather condition effects. Then, 10%–25% of the clear day power output for each PV-DG is applied as the power output for a cloudy day [49], with 5%–10% applied as the power output for a day with overcast skies [50]. The mid-points from the two percent ranges are used, thus 18% of the clear day power output is applied for cloudy days and 8% is applied for overcast days. Fig. 4(a) shows the hour-by-hour estimated power output for a 5 MW PV-DG, where variation in estimated power output for each hour is accounted for depending on the conditions of weather (cloud coverage) on a given day; the profile of power output is similar for a 1 MW and 500 kW PV-DG as well, but with less total output. The impact of the cloud coverage on the power output of PV-DGs is also portrayed in Fig. 4, thus showing why considering the weather uncertainty of a given day within the utility's serviced region is important.

5.2. Critical load power demand

Data used for the power demand of each building type is taken from US Energy Information Administration (EIA) surveys. The surveys provide commercial building power demands for the southern region of the country [51]. Percent sun (%sun) measures how often sunlight hits the ground for a certain geographic area. The %sun measure for the Tennessee area in the case study is 56% [52], and is applied to each building's power demand since the model emphasizes the 6 am–6 pm operation of PV-DG. The uncertainty in power demand for each type of critical load is addressed using the hourly (6 am–6 pm) demand averages provided by the US DoE [53]. We then aggregate the 12 h (6 am–6 pm) demand of each critical load, thus giving us a daily power demand for all buildings. This same demand is applied to each stage (day) of the modeling horizon with the assumption that power demand remains relatively consistent, for each day of the week-long outage, for the critical loads. Fig. 4(b) shows the hour-by-hour estimated power demand for each critical load.

5.3. PV-DG and ESS costs

The following costs (in $/watt) are provided for each size of PV-DG: (1) cost for investing in the PV-DG system ; (2) fixed O&M cost, which signifies the fixed cost of operating and maintaining the PV-DG's availability to provide generation and are estimated as 5% of the investment cost [54]; (3) a cost penalty for excess power penetrated into the network from PV-DG, which is set equal to the cost for investing in the PV-DG system. Since the investment cost is expressed in $/watt (the cost to invest in 1 W of power), we equate this to the excess power penalty as this penalty represents the cost of not using the invested power to supply a building within the network. The cost to invest in a PV-DG system includes the modules and inverter costs, the costs for structural and electrical balance of system components, labor costs for installation, transmission lines and interconnection, taxes and overhead, inspection, permitting, and land acquisition. A comprehensive investment cost, which accounts for the entirety of the microgrid's development, allows us to model the case study microgrid as a fully interconnected and operational system. Though small when compared to the investment and excess power penalty costs, fixed O&M costs are included in the total cost for practical reasons as they help capture the totality of expenses incurred by the utility. Fig. 5 in chart (a) displays the PV-DG costs for each system size.

For the ESSs, we use only one system size (1 MW). Pacific Northwest National Laboratory, operated by the US DoE, states that a 1 MW lithium-ion ESS has an investment cost of $1.88/W and a fixed O&M cost of $0.01/W [55]. The ESS investment costs include the capital costs for energy capacity, power conversion system costs, the balance of plant costs, interconnecting transformers, construction, and commissioning costs [55]. Similar to the PV-DG investment cost, a comprehensive ESS investment cost (accounts for the entirety of ESS development within the microgrid network) allows us to model the ESSs in the case study microgrid as fully connected and functioning in coordination with the PV-DGs within the microgrid.

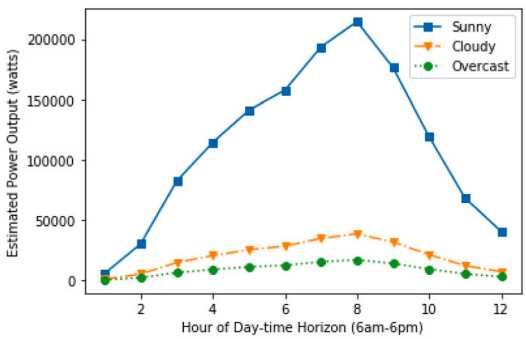

(a) Power output profile by weather.

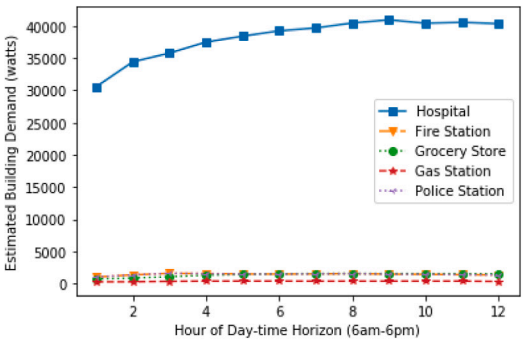

(b) Power demand by building type.

Fig. 4. (a) Estimated power output for a 5 MW PV-DG at each daytime hour based on the type of weather (cloud coverage) experienced that day. Cloudy days output an estimated 18% of the power on Clear days, and Overcast days output an estimated 8% of the power on Clear days; (b) Estimated power demand at each daytime hour based on the building type.

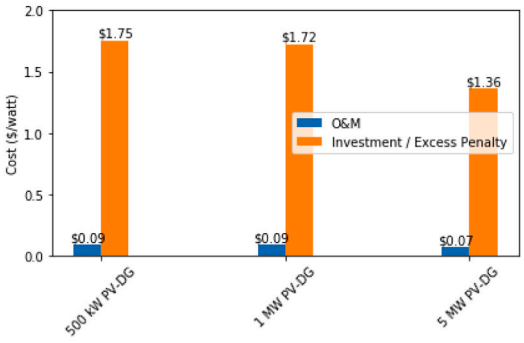

(a) Microgrid PV-DG costs by rated power.

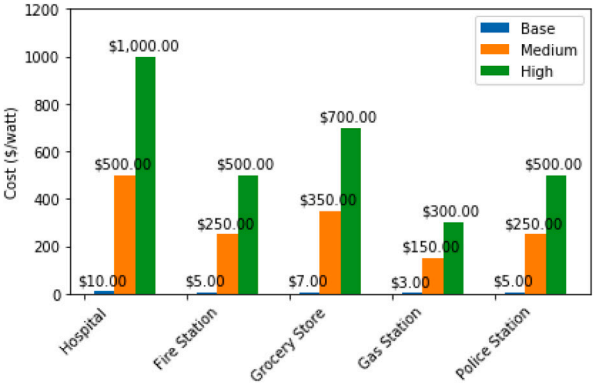

(b) Unmet demand penalty cost by building type.

Fig. 5. Model cost data for investment, operation and maintenance (O&M), excess power penalty, and unmet demand penalty costs. The unmet demand penalty scales are base, medium (50x base) and high (100x base).

5.4. Critical load unmet demand penalty

Each critical load has a cost penalty for power demand that is unmet, which is assigned using an importance hierarchy. The hierarchy of importance for the buildings may change and depends on the specific area the utility services. Utilities using the model can decide which buildings they deem as most important when a widespread blackout occurs, and the established microgrid is switched to island mode operation. The inclusion of the budget constraint puts a limit on how much total power the microgrid can output. Thus, we use the importance hierarchy to help the model decide which critical loads have priority when supplying disaster relief power. The case study assigns the highest priority to hospitals, giving hospitals the largest penalty cost for unmet demand. After the hospitals, grocery stores, police and fire stations, and gas stations are prioritized in that order. Data from EIA surveys shows police and fire stations as having similar demand for power [51]; thus we assigned the two stations the same penalty cost for unmet demand.

Fig. 5, chart (b) displays the penalty cost for unmet demand at each type of building using sensitivity levels of Base, Medium, and High. The sensitivity analysis helps us determine how sensitive the model is to the penalty of unmet demand in the research. We assign a "Base" penalty, where 50x and 100x the "Base" gives the "Medium" and "High" level penalty costs, respectively. There exists no set market rule for what an unmet demand penalty cost should be, and the literature models unmet demand penalties via arbitrarily assigned penalties. Thus, we follow the same approach in this study and set the unmet demand penalty for a hospital, the highest priority building type, at $10.00 for the "Base" penalty level. We determined a penalty of $10.00 through trial and error as a $10.00 penalty proved large enough to demonstrate how the unmet demand penalty impacts the power supply decisions of the model. The remaining building types were assigned unmet demand penalties that scaled the $10.00 assigned to the hospital. Following the importance hierarchy of the buildings, grocery stores were assigned an unmet demand penalty of $7.00, fire and police stations were assigned a $5.00 penalty cost, and gas stations $3.00.

5.5. 5-building and 10-building networks

Our case study uses a 5 and 10-building network in Tennessee. The networks contain the critical loads the Tennessee area utilizes for services essential to the public (e.g., food, safety, transportation and healthcare). For the 5-building network, there is one of each type of critical load (e.g., hospital, grocery store, fire, police and gas station). For the 10-building network, there are two of each type of critical load. The purpose of modeling two different network sizes is to assess how much demand each microgrid budget option can reliably meet/cover over the course of the week-long outage. This allows a utility to determine adequate combinations of budget option and network size for the microgrid.

Recall that the use of a comprehensive DG and ESS investment cost, which accounts for the entirety of the microgrid's development, allows us to model the case study microgrid as a fully connected and operational network. Thus we treat the two microgrid networks as a facility location problem network [37], where the buildings serve as facilities with demand, the DGs and ESSs serve as distribution centers which supply the demand, and the euclidean distance between

Table 2
Optimal solutions of a network composed of 5 critical loads, where PV-DGs are not required within the utility's microgrid. For this specific model, the optimal solutions were witnessed when the Base demand-met penalty is applied for all budget options. The best solution is shown in **bold**.

5 Building & Min DGs = 0 (Base unmet demand penalty)					
Solution result	B = $0M	B = $1M	B = $5M	B = $10M	B = $15M
Solving time (s)	26	25	25	**188**	177
DG location(s)		[4]	[4]		
ESS location(s)			[1, 3]	**[1, 3, 4, 5]**	[1, 3, 4, 5]
Percent of scenarios (3279 total) with 100% demand met	0%	0%	0%	**100%**	100%
DG investment cost	$ –	$ 875,000	$ 875,000	$ –	$ –
ESS investment cost	$ –	$ –	$ 3,760,000	$ **7,520,000**	$ 7,520,000
DG O&M cost	$ –	$ 44,000	$ 44,000	$ –	$ –
ESS O&M cost	$ –	$ –	$ 20,000	$ **40,000**	$ 40,000
Optimal solution	$ 34,155,105	$ 32,009,768	$ 16,775,748	$ **9,976,331**	$ 9,976,331
Q-function solution	$ 34,155,105	$ 31,090,768	$ 12,076,748	$ **2,416,331**	$ 2,416,331
DG power supply efficiency cost	$ –	$ 264,611	$ 264,611	$ –	$ –
ESS power supply efficiency cost	$ –	$ –	$ 785,981	$ **2,416,331**	$ 2,416,333
Excess power cost	$ –	$ –	$ –	$ –	$ –
Unmet demand cost	$ 34,155,105	$ 30,826,156	$ 11,026,156	$ –	$ –
Unmet demand (W)	3,587,320	3,254,425	1,274,425	**0**	0

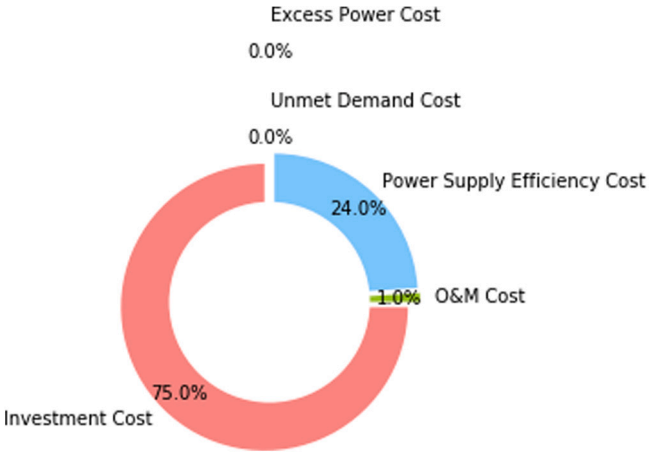

Fig. 6. Pie chart of the optimal solution (objective function), broken down by percentage make-up of each of the cost functions in the objective. This is for a microgrid solution covering a network composed of 5 critical loads, where PV-DGs are not required within the utility's microgrid.

each building and DG/ESS serves as the cost for supply which is also minimized in the objective function.

6. Computational results and discussions

Results for the MS-CFLCP are provided based on the following: (1) the version of MS-CFLCP, where one version of the model does not require a minimum number of PV-DGs to be located within the microgrid and the second version of the model requires a minimum of at least one PV-DG be located as explained in Eq. (2); (2) the size of the utility's serviced network, where one network contains 5 critical loads and the second network contains 10 critical loads; (3) the unmet demand penalty level where the best solution is witnessed. For the two networks analyzed, the 5-building network contains one of each type of critical load and the 10-building network contains two of each type.

6.1. Results for a network of 5 critical loads

The results of the 5-building network, for the model where *minimum DGs located = 0*, are provided in Table 2 with the best solution in **bold**.

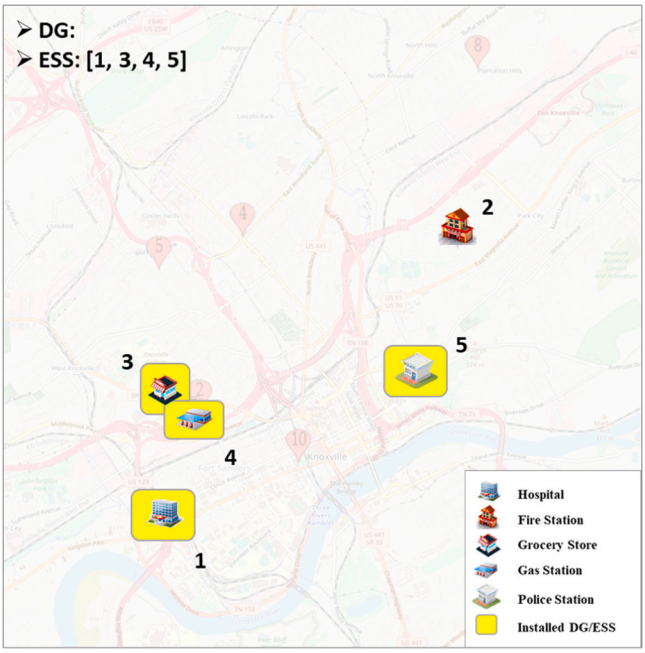

Fig. 7. Visual of where the ESSs are located in the best solution for the 5-building network; results are for the model where *minimum DGs = 0*. Hospitals and Grocery Stores install 5 MW DGs, Fire and Police Stations install 1 MW DGs, Gas Stations install 500 kW DGs and all buildings install 1 MW ESSs.

For a 5-building network, a $10M budget provides the best microgrid solution for the model where *minimum DGs located = 1*. The solution is the same at each level (Base, Medium, and High) of the unmet demand penalty, which shows that the best solution is reached at the Base level without having to utilize the unmet demand penalty to push the model towards optimality. This solution experiences 100% network demand coverage (Unmet Demand Cost = 0) for all 3279 total scenarios, meaning all demand is met for all 5 critical loads in the network for all 7 days of the week-long outage. The $15M budget provides the same solutions, at all three levels of the unmet demand penalty, as the $10M budget. This means a $10M budget is more than enough to reach the most ideal solution (100% demand coverage for all 3279 total scenarios), and that is a solution with no DGs located, 4 ESSs at building IDs 1, 3, 4 and 5, and an optimal solution of $9,976,331 of

Table 3
Optimal solutions of a network composed of 5 critical loads, where a minimum of one PV-DG is required within the utility's microgrid. For this specific model, the optimal solutions were witnessed when the Medium penalty for unmet demand was applied for all budget options; we display the Base level so that the effects of the penalty for unmet demand can be seen as the penalty level increases. The best solution is shown is **bold**.

5 Building & Min DGs = 1 (Medium unmet demand penalty)					
Solution result	B = $0M	B = $1M	B = $5M	B = $10M	B = $15M
Solving time (s)	25	25	421	**366**	325
DG location(s) ESS location(s)		[4]	[4] [1, 3]	**[4]** **[1, 3, 4, 5]**	[4] [1, 3, 4, 5]
Percent of scenarios (3279 total) with 100% demand met	0%	0%	0%	**100%**	100%
DG investment cost	$ –	$ 875,000	$ 875,000	$ **875,000**	$ 875,000
ESS investment cost	$ –	$ –	$ 3,760,000	$ **7,520,000**	$ 7,520,000
DG O&M cost	$ –	$ 44,000	$ 44,000	$ **44,000**	$ 44,000
ESS O&M cost	$ –	$ –	$ 20,000	$ **40,000**	$ 40,000
Optimal solution	$ 1,707,755,243	$ 1,542,491,420	$ 557,057,398	$ **10,489,545**	$ 10,489,544
Q-function solution	$ 1,707,755,243	$ 1,541,572,420	$ 552,358,398	$ **2,010,545**	$ 2,010,544
DG power supply efficiency cost	$ –	$ 264,611	$ 264,611	$ **217,841**	$ 218,777
ESS power supply efficiency cost	$ –	$ –	$ 785,981	$ **1,792,704**	$ 1,791,768
Excess power cost	$ –	$ –	$ –	$ –	$ –
Unmet demand cost	$ 1,707,755,243	$ 1,541,307,809	$ 551,307,809	$ –	$ –
Unmet demand (W)	3,587,320	3,254,425	1,274,425	**0**	0
5 Building & Min DGs = 1 (Base unmet demand penalty)					
Solution result	B = $0M	B = $1M	B = $5M	B = $10M	B = $15M
Solving time (s)	26	25	216	259	306
DG location(s) ESS location(s)		[4]	[4] [1, 3]	[4] [1, 3, 4]	[4] [1, 3, 4]
Percent of scenarios (3279 total) with 100% demand met	0%	0%	0%	35%	35%
DG investment cost	$ –	$ 875,000	$ 875,000	$ 875,000	$ 875,000
ESS investment cost	$ –	$ –	$ 3,760,000	$ 5,640,000	$ 5,640,000
DG O&M cost	$ –	$ 44,000	$ 44,000	$ 44,000	$ 44,000
ESS O&M cost	$ –	$ –	$ 20,000	$ 30,000	$ 30,000
Optimal solution	$ 34,155,105	$ 32,009,768	$ 16,775,748	$ 10,097,904	$ 10,097,903
Q-function solution	$ 34,155,105	$ 31,090,768	$ 12,076,748	$ 3,508,904	$ 3,508,903
DG power supply efficiency cost	$ –	$ 264,611	$ 264,611	$ 262,713	$ 262,490
ESS power supply efficiency cost	$ –	$ –	$ 785,981	$ 1,525,583	$ 1,525,806
Excess power cost	$ –	$ –	$ –	$ –	$ –
Unmet demand cost	$ 34,155,105	$ 30,826,156	$ 11,026,156	$ 1,720,612	$ 1,720,612
Unmet demand (W)	3,587,320	3,254,425	1,274,425	302,373	302,373

which $7.5M (about 75% of optimal solution/total cost) is investment costs for the 4 ESSs. Fig. 6 displays a breakdown of how much of the optimal solution (objective function) each cost function makes up; the desire is for the optimal solution (objective function) to be primarily composed of the investment and power supply costs as these are the only major costs that cannot be minimized to 0 within the model. We see the desired outlook for the chart in Fig. 6 where the unmet demand and excess power cost are both at 0%, signifying an ideal solution. Fig. 7 shows the location of the four ESSs in the best solution for the 5-building network (minimum DGs = 0).

The results of the 5-building network, for the model where *minimum DGs located = 1*, are provided in Table 3 with the best solution in **bold**. Similar to the model where *minimum DGs located = 0*, a $10M budget provides the best solution for the model where *minimum DGs located = 1*. For this model, however, it is when the Medium level penalty for unmet demand is applied (with a $10M budget) that we see the best solution. The Base level solution, with a $10M budget, experiences 100% network demand coverage (Unmet Demand Cost = 0) for 1159 of the 3279 total scenarios (35%). The Medium level of the unmet demand penalty pushes the model to 100% network demand coverage for all 3279 scenarios. The $15M budget provides the same solutions, at all three unmet demand penalty levels, as the $10M budget. This means a $10M budget is more than enough to reach the ideal solution (100% demand coverage for all 3279 total scenarios), and that is a solution

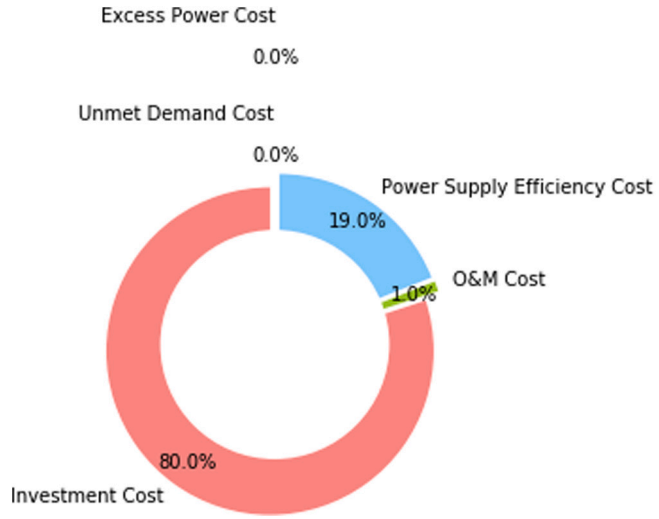

Fig. 8. Pie chart of the optimal solution (objective function), broken down by percentage make-up of each of the cost functions in the objective. This is for a microgrid solution covering a network composed of 5 critical loads, where a minimum of one PV-DG is required within the utility's microgrid.

with 1 DG located at building ID 4, 4 ESSs at building IDs 1, 3, 4 and 5, and an optimal solution of $10,489,545 of which $8.4M (about 80% of optimal solution/total cost) is investment costs for the 1 DG and 4 ESSs. Fig. 8 displays a breakdown of how much of the optimal solution (objective function) each cost function makes up; the desire is for the optimal solution (objective function) to be primarily composed of the investment and power supply costs as these are the only major costs that cannot be minimized to 0 within the model. As with the first 5-building network model, we again see the desired outlook for the chart in Fig. 8 where the unmet demand and excess power cost are both at 0%, signifying an ideal solution.

6.1.1. Effects of the unmet demand and excess power penalties (5-building)

The effects of the unmet demand penalty (applied in the objective's 4th cost function, which minimizes unmet demand and unmet demand costs within the microgrid) are shown in the Table 3 results. For the model requiring DG location (Minimum DGs Located = 1 model), the Base level solutions for the $10M and $15M budgets locate a total of $6.5M (total investment) in DGs and ESSs (DG = 4 and ESS = 1, 3, 4) versus a total of $8.4M (total investment) in DGs and ESSs (DG = 4 and ESS = 1, 3, 4, 5) located at the Medium level solutions. This is because the model found it cheaper to incur the additional investment costs of $1.9M in DGs and ESSs within the microgrid to help alleviate the total unmet demand experienced with the Medium level penalty versus those experienced at the Base level penalty. The additional $1.9M reduced total unmet demand from 302,373 W to 0 W, and increased the number of scenarios where 100% network demand coverage is experienced from 35% (at the Base level for the $10M and $15M budget options) to an ideal 100% (at the Medium level for the $10M and $15M budget options) of the 3279 total scenarios. When the High level penalty is applied, the best solution for a $10M and $15M budgets remains the same (DG = 4 and ESS = 1, 3, 4, 5), which means that the Medium level penalty achieves the best solution for all levels when given a $10M or $15M budget. What changes from the Base to Medium level is the addition of another ESS at building ID 5. When the penalty scale moves to the Medium level, more power output is required to help alleviate the total unmet demand experienced in the network, and thus the model locates another ESS at building ID 5. Locating the ESS at building ID 5 adds an additional 1 MW of stored power and an additional $1.9M to the total investment cost. However, the additional $1.9M helped reduce the total unmet demand to 0 W, giving us a fully covered network (100% demand coverage for all 3279 total scenarios) for the entire week-long outage.

The effects of the excess power penalty (applied in the objective's 5th cost function which minimizes the excess renewable power within the microgrid) are shown by the resulting $0 in excess power costs for all solutions across all budgets in both models. This means that the applied excess penalty costs ensured that the DGs and ESSs located in each solution provided enough power to, at most, meet the demand of the network. We never witness a solution where the installed DGs and ESSs provided more power to the network than what the network has in demand. Thus, we see how applying an excess power penalty cost benefits the microgrid and main grid by ensuring issues such as utility-scale reverse power flow (which is caused by excess renewable generation and has system functionality consequences such as voltage peaks and reduced power quality [40]) do not occur within the designed microgrid network and do not increase the optimal solution of the microgrid.

6.1.2. Minimum DG vs. no minimum DG model (5-building)

The difference in the two models is shown when comparing Tables 2 and 3. One model contains a constraint that requires at least 1 DG to be located within the microgrid, while the other model does not contain this constraint. We see that, for the $10M and $15M budget options, the model where minimum DGs located = 0 finds it more cost effective to locate just ESSs and NO DGs at all within the microgrid. This is made possible due to this model not containing the constraint that requires at least 1 DG to be located. These are the only budget options, across both models, where NO DGs are located at all (disregarding the $0 investment which by default would not have any DGs or ESSs located due to a budget of $0). Utilities that service heavily clear regions may want to mandate that their microgrid contains at least one DG so that they can take advantage of the predominantly clear weather (cloud coverage) of the region. On the other hand, utilities that service regions with a lesser number of annual clear days may not find it as useful to require a DG in the microgrid due to the added expense the DG would bring if the ESSs are enough to meet demand. By providing both models, we allow utilities the flexibility of deciding based upon the clear weather (cloud coverage) regularity of their serviced regions.

6.2. Results for a network of 10 critical loads

The results of the 10-building network, for the model where *minimum DGs located = 0*, are provided in Table 4 with the best solution in **bold**. For a 10-building network, a $15M budget at the Medium level of the unmet demand penalty, provides the best solution for the model where minimum DGs located = 0. This solution experiences 100% network demand coverage (Unmet Demand Cost = 0) for 3192 of the 3279 total scenarios (97%). The $15M budget option at the Base level produces a lower optimal solution ($18,459,884) than this solution ($19,729,118) but only experiences 0 unmet demand for 86% of the 3279 total scenarios, whereas this solution experiences 0 unmet demand for 97% of the 3279 total scenarios. The Medium level for the $15M budget option has a slightly higher investment cost ($14.9M) than the Base level for the $15M budget option ($14.0M), but both investments costs fall within the $15M budget provided. The solution results in a 1 MW DG located at building ID 10 and ESSs located at building IDs 1, 2, 5, 6, 7, 9 and 10.

The results of the 10-building network, for the model where *minimum DGs located = 1*, are provided in Table 5 with the best solution in **bold**. The best solution for the model where minimum DGs located = 1 is identical to the best solution for the model where minimum DGs located = 0, and is witnessed with a $15M budget when the Medium unmet demand penalty is applied. The solution experiences 100% network demand coverage (Unmet Demand Cost = 0) for 3192 of the 3279 total scenarios (97%) just as was experienced in the model where the minimum DGs located = 0. The DGs and ESSs located, as well as the costs and optimal solution are also similar between both model solutions. Fig. 9 displays a breakdown of how much of the optimal solution (objective function) each cost function makes up; the desire is for the optimal solution (objective function) to be primarily composed of the investment and power supply costs as these are the only major costs that cannot be minimized to 0 within the model. We do not see the desired outlook for the chart in Fig. 9 as 3% of the optimal solution is unmet demand costs. Thus, unlike the 5-building network microgrid solution, the increased demand of the 10-building network does not lead to an ideal microgrid solution where 100% of the network demand is covered. Fig. 10 shows the location of the one DG and seven ESSs in the best solution for the 10-building network (both models, where minimum DGs = 0 and 1, reached equivalent best solutions).

Since the best microgrid solution for a network of 10 critical loads only reaches 100% demand coverage for 97% of the 3279 scenarios, we portray the unmet demand for the worst-case week - a week where each of the 7 days experiences overcast weather (cloud coverage) and the PV-DGs output the least amount of power into the microgrid — in Fig. 11. Fig. 11 shows 0% unmet demand for days 1–4 of the worst-case week, which is ideal. By day 5 and 6, the microgrid experiences 1% unmet demand and 8% unmet demand by day 7.

Table 4
Optimal solutions of a network composed of 10 critical loads, where PV-DGs are not required within the utility's microgrid. For this specific model, the optimal solutions were witnessed when the Medium penalty for unmet demand was applied for all budget options; we display the Base level so that the effects of penalty can be seen as the penalty level increases. The best solution is shown in **bold**.

10 Building & Min DGs = 0 (Medium unmet demand penalty)					
Solution result	B = $0M	B = $1M	B = $5M	B = $10M	B = $15M
Solving time (s)	53	54	54	380	**3587**
DG location(s)		[7]	[7]		**[10]**
ESS location(s)			[1, 2]	[1, 2, 6, 7, 10]	**[1, 2, 5, 6, 7, 9, 10]**
Percent of scenarios (3279 total) with 100% demand met	0%	0%	0%	0%	**97%**
DG investment cost	$ –	$ 875,000	$ 875,000	$ –	$ **1,720,000**
ESS investment cost	$ –	$ –	$ 3,760,000	$ 9,400,000	$ **13,160,000**
DG O&M cost	$ –	$ 44,000	$ 44,000	$ –	$ **86,000**
ESS O&M cost	$ –	$ –	$ 20,000	$ 50,000	$ **70,000**
Optimal solution	$ 3,415,510,485	$ 3,250,040,743	$ 2,263,820,743	$ 951,340,510	$ **19,729,118**
Q-function solution	$ 3,415,510,485	$ 3,249,121,743	$ 2,259,121,743	$ 941,890,510	$ **4,693,118**
DG power supply efficiency cost	$ –	$ 58,692	$ 58,692	$ –	$ **659,072**
ESS power supply efficiency cost	$ –	$ –	$ –	$ 1,380,025	$ **3,368,690**
Excess power cost	$ –	$ –	$ –	$ –	$ –
Unmet demand cost	$ 3,415,510,485	$ 3,249,063,051	$ 2,259,063,051	$ 940,510,485	$ **665,357**
Unmet demand (W)	7,174,640	6,841,745	4,861,745	2,224,640	**3226**
10 Building & Min DGs = 0 (Base unmet demand penalty)					
Solution result	B = $0M	B = $1M	B = $5M	B = $10M	B = $15M
Solving time (s)	53	54	53	402	2714
DG location(s)		[7]	[7]		[7]
ESS location(s)			[1, 2]	[1, 2, 6, 7, 10]	[1, 2, 4, 5, 6, 7, 10]
Percent of scenarios (3279 total) with 100% demand met	0%	0%	0%	0%	86%
DG investment cost	$ –	$ 875,000	$ 875,000	$ –	$ 875,000
ESS investment cost	$ –	$ –	$ 3,760,000	$ 9,400,000	$ 13,160,000
DG O&M cost	$ –	$ 44,000	$ 44,000	$ –	$ 44,000
ESS O&M cost	$ –	$ –	$ 20,000	$ 50,000	$ 70,000
Optimal solution	$ 68,310,210	$ 65,958,953	$ 49,938,953	$ 29,640,234	$ 18,459,884
Q-function solution	$ 68,310,210	$ 65,039,953	$ 45,239,953	$ 20,190,234	$ 4,310,884
DG power supply efficiency cost	$ –	$ 58,692	$ 58,692	$ –	$ 84,566
ESS power supply efficiency cost	$ –	$ –	$ –	$ 1,380,025	$ 4,122,267
Excess power cost	$ –	$ –	$ –	$ –	$ –
Unmet demand cost	$ 68,310,210	$ 64,981,261	$ 45,181,261	$ 18,810,210	$ 104,062
Unmet demand (W)	7,174,640	6,841,745	4,861,745	2,224,640	26,726

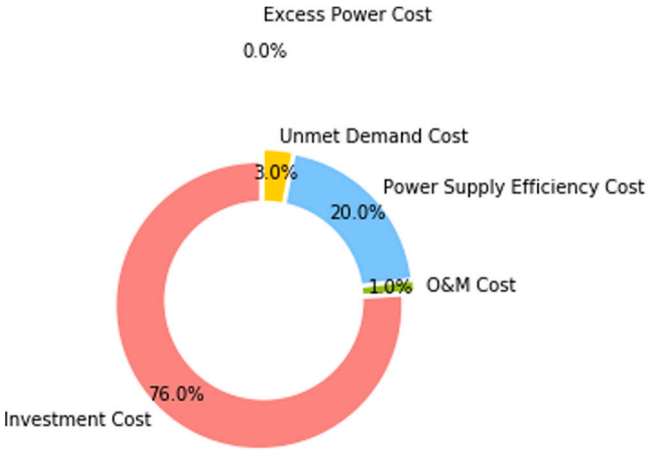

Fig. 9. Pie chart of the optimal solution (objective function), broken down by percentage make-up of each of the cost functions in the objective. This is for a microgrid solution covering a network composed of 10 critical loads, regardless of minimum DG requirements. Ideally, investment and power supply costs should make up the majority of the chart as these are the only major costs that cannot be minimized to 0.

6.2.1. Effects of the unmet demand and excess power penalties (10-building)

The effects of the unmet demand penalty (applied in the objective's 4th cost function which minimizes unmet demand and unmet demand costs within the microgrid) witnessed in Table 3 are also seen in the Table 5 results. For the model requiring DG location (minimum DGs Located = 1 model), the Base level solution for the $10M budget locates a total of $9.2M in DGs and ESS (DG = 10 and ESS = 1, 2, 6, 7) versus a total of $9.9M in DGs and ESS (DG = 4, 7, 10 and ESS = 1, 2, 7) located at the Medium level. This is because the model found it cheaper to incur the additional investment costs of $715,000 in DGs and ESSs within the microgrid to help alleviate the total unmet demand experienced at the Medium level penalty versus that at the Base level penalty (additional $715,000 reduced total unmet demand by 2,548,851–2,541,192 = 7659 W); 7659 W is enough wattage to power a gas station for 2 daytime periods (12 daytime hours x 2 days). When the High level penalty is applied, the best solution for a $10M budget remains the same (DG = 4, 7, 10 and ESS = 1, 2, 7), which means that the Medium level penalty achieves the optimal solution for all levels when given a $10M budget. We see the unmet demand penalty effects again for the $15M budget of both models where the Base level solution locates a total of $14.0M in DGs and ESSs versus a total of $14.8M. This is because the Base level solutions locate a smaller 500 kW DG at building ID 7. When the penalty scale moves

Table 5
Optimal solutions of a network composed of 10 critical loads, where a minimum of one PV-DG is required within the utility's microgrid. For this specific model, the optimal solutions were witnessed when the Medium penalty for unmet demand was applied for all budget options; we display the Base level so that the effects of the penalty can be seen as the penalty level increases. The best solution is shown in **bold**.

10 Building & Min DGs = 1 (Medium unmet demand penalty)					
Solution result	B = $0M	B = $1M	B = $5M	B = $10M	B = $15M
Solving time (s)	53	80	691	30,018	**2440**
DG location(s) ESS location(s)		[7]	[7] [1, 2]	[4, 7, 10] [1, 2, 7]	**[10]** **[1, 2, 5, 6, 7, 9, 10]**
Percent of scenarios (3279 total) with 100% demand met	0%	0%	0%	1%	**97%**
DG investment cost	$ –	$ 875,000	$ 875,000	$ 4,315,000	$ **1,720,000**
ESS investment cost	$ –	$ –	$ 3,760,000	$ 5,640,000	$ **13,160,000**
DG O&M cost	$ –	$ 44,000	$ 44,000	$ 216,000	$ **86,000**
ESS O&M cost	$ –	$ –	$ 20,000	$ 30,000	$ **70,000**
Optimal solution	$ 3,415,510,485	$ 3,250,040,743	$ 2,263,820,743	$ 1,111,186,198	$ **19,729,117**
Q-function solution	$ 3,415,510,485	$ 3,249,121,743	$ 2,259,121,743	$ 1,100,985,198	$ **4,693,117**
DG power supply efficiency cost	$ –	$ 58,692	$ 58,692	$ 1,659,926	$ **660,074**
ESS power supply efficiency cost	$ –	$ –	$ –	$ 245,420	$ **3,367,688**
Excess power cost	$ –	$ –	$ –	$ –	$ –
Unmet demand cost	$ 3,415,510,485	$ 3,249,063,051	$ 2,259,063,051	$ 1,099,079,854	$ **665,357**
Unmet demand (W)	7,174,640	6,841,745	4,861,745	2,541,192	**3226**
10 Building & Min DGs = 1 (Base unmet demand penalty)					
Solution result	B = $0M	B = $1M	B = $5M	B = $10M	B = $15M
Solving time (s)	53	78	511	1097	2547
DG location(s) ESS location(s)		[7]	[7] [1, 2]	[10] [1, 2, 6, 7]	[7] [1, 2, 4, 5, 6, 7, 10]
Percent of scenarios (3279 total) with 100% demand met	0%	0%	0%	0%	86%
DG investment cost	$ –	$ 875,000	$ 875,000	$ 1,720,000	$ 875,000
ESS investment cost	$ –	$ –	$ 3,760,000	$ 7,520,000	$ 13,160,000
DG O&M cost	$ –	$ 44,000	$ 44,000	$ 86,000	$ 44,000
ESS O&M cost	$ –	$ –	$ 20,000	$ 40,000	$ 70,000
Optimal solution	$ 68,310,210	$ 65,958,953	$ 49,938,953	$ 32,438,655	$ 18,459,889
Q-function solution	$ 68,310,210	$ 65,039,953	$ 45,239,953	$ 23,072,655	$ 4,310,889
DG power supply efficiency cost	$ –	$ 58,692	$ 58,692	$ 661,763	$ 94,531
ESS power supply efficiency cost	$ –	$ –	$ –	$ 358,573	$ 4,111,931
Excess power cost	$ –	$ –	$ –	$ –	$ –
Unmet demand cost	$ 68,310,210	$ 64,981,261	$ 45,181,261	$ 22,052,322	$ 104,437
Unmet demand (W)	7,174,640	6,841,745	4,861,745	2,548,851	26,880

to the Medium level, more power output is required to help alleviate the total unmet demand experienced in the network, and thus a larger (1 MW) DG is located at building ID 10 instead of the 500 kW seen in the Base level solution. Locating the 1 MW DG at building ID 10 adds an additional $845,000 to the total investment cost, but the additional $845,000 helps to reduce the total unmet demand by 26,880–3226 = 23,654 W); 23,654 W is enough wattage to power a grocery store for 1 daytime period (12 daytime hours) and a gas station for 2 daytime periods (12 daytime hours x 2 days). This increases the number of scenarios where 100% demand coverage is witnessed from 86% (at the Base level, $15M) to 97% (at the Medium level, $15M) of the 3279 total scenarios.

The results in Tables 4 and 5 also show how the unmet demand penalty affects of the objective's 3rd cost function, which minimizes distribution power losses by reducing the distance traveled for power supply, thus improving power supply efficiency. At the $15M budget for the Base level (both models), we see ESSs located at building IDs 1, 2, 4, 5, 6, 7 and 10. Then, at the Medium level, the ESS at building ID 4 is replaced by an ESS at building ID 9. This occurs due to the increase in unmet demand penalty cost. As the penalty cost for unmet demand increases, the model looks to minimize the optimal solution by minimizing another cost function of the objective, and in this case, it is the distance for power supply cost function. Since all ESSs have the same capacity of 1 MW, the change between the building IDs where an ESS is located at the Base and Medium levels of the $15M budget occur due to the model minimizing the distance traveled for power supply to help alleviate the overall optimal solution of the model. This change, along with the larger DG at building ID 10 versus ID 7, helps reduce the ESS power supply cost from $4.1M at the Base level to $3.3M at the Medium level solution for the $15M budget option.

As we saw in the 5-building network microgrid solution, the effects of the excess power penalty are again shown by the resulting $0 in excess power costs across all microgrid solutions for both models. We again see how applying an excess power penalty cost benefits the microgrid system by ensuring issues such as utility-scale reverse power flow (which is caused by excess renewable generation and has system functionality consequences [40]) do not increase the optimal solution of the microgrid or potentially cause issues such as voltage peaks and reduced power quality within the system.

6.2.2. Minimum DG vs. no minimum DG model (10-building)

As with the 5-building microgrid solutions, we see the difference in the two models by comparing the results of the 10-building microgrid solutions in Tables 4 and 5. We see that, for the $10M budget option, the model where minimum DGs located = 0 model finds it more cost effective to locate just ESSs and NO DGs at all within the microgrid. This happens to be the only budget option across both models for the 10-building network, where no DGs are located at all (disregarding

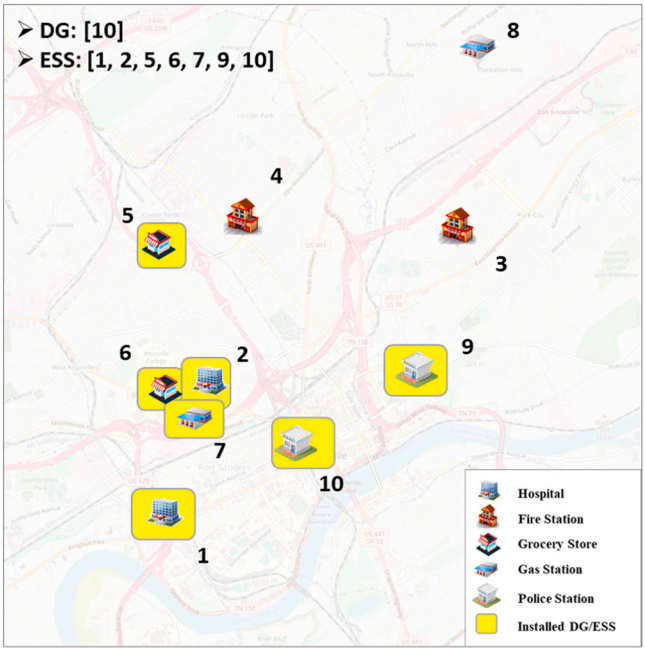

Fig. 10. Illustration of the DG and ESSs locations in the optimal solution for the 10-building network. Results are the same for both models (*minimum DGs = 0 and 1)*, *i.e.*, with or without DG requirement for ESSs. Hospitals and Grocery Stores install 5 MW DGs, Fire and Police Stations install 1 MW DGs, Gas Stations install 500 kW DGs and all buildings install 1 MW ESSs.

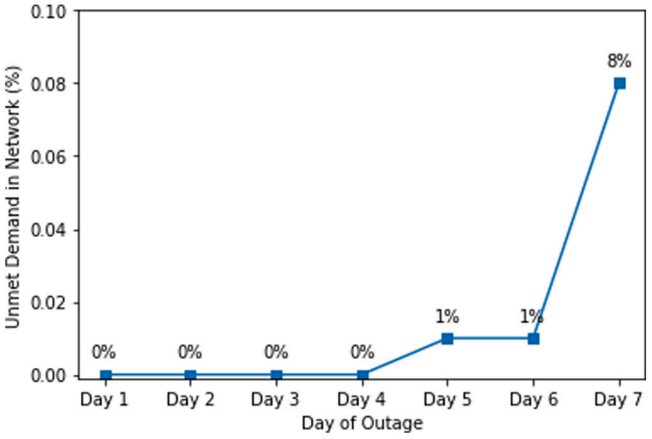

Fig. 11. Daily unmet demand for the worst-case week-long outage, which is a week with overcast skies (least PV-DG output) every day of the week-long outage. Demand is fully met until days 5–7 of the week.

the $0 investment, which by default would not have any DGs or ESSs located due to a budget of $0). As previously stated, by providing both models, we allow utility flexibility to decide which model best applies to their serviced region based upon the clear weather (cloud coverage) regularity of the region.

6.3. ROIs for microgrid solution (5-building and 10-building networks)

Return on Investment (ROI) is a performance measure used to evaluate the efficiency of an investment or compare the efficiency of a number of different investments. The ROI denominator is the total investment cost of the DGs+ESSs of each solution (given budget options of $0M, $1M, $5M, $10M, or $15M). The ROI numerator is the "returns", which are what the utility gains by investing $X millions into a microgrid. We define "returns" as the critical loads experiencing uninterrupted power supply during the week-long power outage caused by the natural disaster as this is the focus of the model and research. The returns are computed by subtracting the optimal solution (minimized total cost of the objective function) of a $1, $5, $10, or $15M budget option, from the optimal solution if the utility does not invest in a microgrid at all ($0M budget option). We then divide this subtracted value by the total investment cost (DG+ESS investment cost) of the $1, $5, $10, or $15M budget option. Every budget option should return an ROI greater than 100% as any microgrid, whether a small one with less than $1M invested or a larger one, will provide more power into the network than no microgrid at all ($0M budget option) as we are modeling a situation with the microgrid islanded as the only power source for the critical loads within the network. Thus, the goal would be to determine how much more return each investment amount provides when compared to another investment amount.

Tables 6 and 7 display the ROIs for a microgrid solution covering a network of 5 critical loads with and without a minimum of one PV-DG within the microgrid, respectively. For the results in Table 6, the highest ROI is 375% and is achieved by the $5M budget option. However, based on optimal solutions, the best solution from Table 6 occurs when a $10M budget is provided and results in an ROI of 322%. For the results in Table 7, the best solution is reached when the Medium penalty for unmet demand is applied (see Table 3). Thus, the ROI is also affected by the Medium level penalty and results in the large ROI outcome of 20218%.

Tables 8 and 9 display the ROIs for a microgrid solution covering a network of 10 critical loads with and without a minimum of one PV-DG within the microgrid, respectively. For the results in both Tables 8 and 9, the best solution is reached at the Medium level of the unmet demand penalty (see Tables 4 and 5); the two models reached identical best solutions. We see another large ROI outcome of 22821% for both solutions due to the effects of the Medium level penalty.

In all four ROI result tables, the best solution's ROI (written in **bold**) is less than the highest ROI. This difference can be attributed to a larger DG+ESS investment (denominator of ROI equation) for the best solutions versus that of the solutions with the highest ROI. Using Table 6 as an example, the difference in the 375% ROI (the highest ROI of the solutions) and the 322% ROI (the ROI of the best solution) is caused by a larger DG+ESS investment (denominator of ROI equation) for the $10M budget (about $7.5M) versus that of the $5M budget (about $4.6M). The same situation can be seen for the results in Tables 7–9.

7. Conclusion, limitations and future research

We develop a multi-stage stochastic program that models the investment economics, reliability, and resilience of a utility-owned microgrid operating in island mode due to natural disaster-caused damage to the main grid. We model a situation where the main grid damage has caused a week-long power outage, and the microgrid is used by the utility to provide disaster relief power supply to the critical loads within the utility's serviced region. The microgrid model uses photovoltaic distributed generators (PV-DGs) and energy storage systems, while accounting for the hourly uncertainty and weather (cloud coverage) uncertainty in PV-DG power output. The nested L-shaped method is used to solve the multi-stage stochastic program, and a holistic objective function that captures the investment, operation and maintenance, power supply efficiency, reliability, and resilience of the microgrid in terms of a minimized total cost to the utility is provided. We consider the budgetary limitations of a utility when establishing such a microgrid and thus limit the investment costs to allocated budget amounts.

The model is applied to a case study resulting in an exhaustive solution that analyzes the microgrid's reliability performance across 3279 scenarios of a week-long power outage, where each scenario is a combination of the day of the outage (7 days total) and the weather

Table 6
Each investment's Return on Investment (ROI) displayed by budget option for a microgrid solution covering a network composed of 5 critical loads, where PV-DGs are not required within the utility's microgrid. The best solution is shown in **bold**.

5 Buildings & Min DGs = 0 (Base unmet demand penalty)		
DG+ESS investment (Budget)	Optimal solution	ROI of investment
$0 ($0M)	$ 34,155,105	0%
$875,00 ($1M)	$ 32,009,768	245%
$4,635,000 ($5M)	$ 16,775,748	375%
$7,520,000 ($10M)	$ **9,976,331**	**322%**
$7,520,000 ($15M)	$ 9,976,331	322%

Table 7
Each investment's Return on Investment (ROI) displayed by budget option for a microgrid solution covering a network composed of 5 critical loads, where a minimum of one PV-DG is required within the utility's microgrid. The best solution is shown in **bold**, and is reached when the Medium penalty for unmet demand; we display the Base level so that the effects of the penalty can be seen as the penalty level increases.

5 Buildings & Min DGs = 1 (Medium unmet demand penalty)		
DG+ESS investment (Budget)	Optimal solution	ROI of investment
$0 ($0M)	$ 1,707,755,243	0%
$875,000 ($1M)	$ 1,542,491,420	18 887%
$4,635,000 ($5M)	$ 557,057,398	24 826%
$8,395,000 ($10M)	$ **10,489,545**	**20 218%**
$8,395,000 ($15M)	$ 10,489,544	20 218%
5 Buildings & Min DGs = 1 (Base unmet demand penalty)		
DG+ESS investment (Budget)	Optimal solution	ROI of investment
$0 ($0M)	$ 34,155,105	0%
$875,000 ($1M)	$ 32,009,768	245%
$4,635,000 ($5M)	$ 16,775,748	375%
$6,515,000 ($10M)	$ 10,097,904	369%
$6,515,000 ($15M)	$ 10,097,903	369%

Table 8
Each investment's Return on Investment (ROI) displayed by budget option for a microgrid solution covering a network composed of 10 critical loads, where PV-DGs are not required within the utility's microgrid. The best solution is shown in **bold**, and is reached when the Medium penalty for unmet demand; we display the Base level so that the effects of the unmet demand penalty can be seen as the penalty level increases.

10 Buildings & Min DGs = 0 (Medium unmet demand penalty)		
DG+ESS investment (Budget)	Optimal solution	ROI of investment
$0 ($0M)	$ 3,415,510,485	0%
$875,000 ($1M)	$ 3,250,040,743	18 911%
$4,635,000 ($5M)	$ 2,263,820,743	24 848%
$9,400,000 ($10M)	$ 951,340,510	26 215%
$14,880,000 ($15M)	$ **19,729,118**	**22 821%**
10 Buildings & Min DGs = 0 (Base unmet demand penalty)		
DG+ESS investment (Budget)	Optimal solution	ROI of investment
$0 ($0M)	$ 68,310,210	0%
$875,000 ($1M)	$ 65,958,953	269%
$4,635,000 ($5M)	$ 49,938,953	396%
$9,400,000 ($10M)	$ 29,640,234	411%
$14,035,000 ($15M)	$ 18,459,884	355%

witnessed that day (e.g., clear, cloudy or overcast cloud coverage). Solutions to the model provide the optimal location, size, power supply assignment, and the total number of DGs and ESSs within the utility-owned microgrid. Results of the model show that an islanded utility-scale microgrid can effectively provide power supply to a network of 5 and 10 critical loads, with 100% and 97% of the scenarios experiencing full demand coverage, respectively, over the duration of a week-long power outage. The full development of such microgrids requires investments of $7.5M and $14.8M for the 5 and 10-building networks, respectively.

The developed model has limitations relating to the building demand used and the modeling horizon. The demand data of the buildings in each stage (day) is a sum of each building's daytime demand from 6:00 AM to 6:00 PM. We account for only the daytime demand due to the microgrid functioning with the use of PV-DGs that require sunlight. nighttime demand of the buildings is handled by the back-up generators we assume each building possesses. Future work can remove the assumption that the buildings possess back-up generators and develop the microgrid model to account for the nighttime demand of the buildings as well. In regards to the modeling horizon, each stage equates to a 12 h day. However, natural disaster-caused power outages can last only hours, and thus, an hour-by-hour analysis of the developed model would be beneficial. Breaking 7 days into an hour-by-hour analysis (168 h or 168 stages) would lead to unreasonably long computation time with the current model. Thus, future work can be done to investigate the use of simulation software to solve the developed model as simulations can handle much longer modeling horizons.

CRediT authorship contribution statement

Rodney Kizito: Conceptualization, Methodology, Software, Data curation, Writing – original draft. **Zeyu Liu:** Methodology, Modeling, Writing – review & editing, Software. **Xueping Li:** Conceptualization,

Table 9
Each investment's Return on Investment (ROI) displayed by budget option for a microgrid solution covering a network composed of 10 critical loads, where a minimum of one PV-DG is required within the utility's microgrid. The best solution is shown in **bold**, and is reached when the Medium penalty for unmet demand is applied; we display the Base level so that the effects of the unmet demand penalty can be seen as the penalty level increases.

10 Buildings & Min DGs = 1 (Medium unmet demand penalty)		
DG+ESS investment (Budget)	Optimal solution	ROI of investment
$0 ($0M)	$ 3,415,510,485	0%
$875,000 ($1M)	$ 3,250,040,743	18 911%
$4,635,000 ($5M)	$ 2,263,820,743	24 848%
$9,955,000 ($10M)	$ 1,111,186,198	23 147%
$14,880,000 ($15M)	**$ 19,729,117**	**22 821%**
10 Buildings & Min DGs = 1 (Base unmet demand penalty)		
DG+ESS investment (Budget)	Optimal solution	ROI of investment
$0 ($0M)	$ 68,310,210	0%
$875,000 ($1M)	$ 65,958,953	269%
$4,635,000 ($5M)	$ 49,938,953	396%
$9,240,000 ($10M)	$ 32,438,655	388%
$14,035,000 ($15M)	$ 18,459,889	355%

Funding acquisition, Supervision, Writing – Review & editing. **Kai Sun:** Conceptualization.

Declaration of competing interest

The authors declare that they have no known competing financial interests or personal relationships that could have appeared to influence the work reported in this paper.

Acknowledgments

This work was supported in part by the Chad/Ann Blair Holliday Fellowship, awarded by the Department of Industrial & Systems at the University of Tennessee, Knoxville, United States.

References

[1] Shield SA, Quiring SM, Pino JV, Buckstaff K. Major impacts of weather events on the electrical power delivery system in the United States. Energy 2021;218:119434.
[2] Leslie M. Texas crisis highlights grid vulnerabilities. 2021.
[3] Barr D, Carr C, Putnam E. Microgrid Effects and Opportunities for Utilities. Technical report, Kansas City, MO: Burns & McDonnell; 2016.
[4] Weir W. When power generator fails, hospital takes extreme measure of evacuation. 2011, https://www.courant.com/health/hc-xpm-2011-08-29-hc-jmh-hurricane-evacuation-0830-20110829-story.html.
[5] Light J. Generators failed at two hospitals during blackout. San Diego Union-Tribune 2011.
[6] D'Onofrio. Chicago weather: Flooding, power outage force evacuation of Northwestern Lake Forest Hospital. 2017, https://abc7chicago.com/chicago-weather-flooding-standing-water-stranded/2208536/.
[7] Harkins. Storm damage, power outage causes claremore hospital partial evacuation. 2020, https://tulsaworld.com/news/state-and-regional/storm-damage-power-outage-causes-claremore-hospital-partial-evacuation/article_660f0ffd-8627-5de8-918c-3c65aa0f1405.html.
[8] Fink S. The deadly choices at memorial. 2009, https://www.propublica.org/article/the-deadly-choices-at-memorial-826.
[9] Hirsch A, Parag Y, Guerrero J. Microgrids: A review of technologies, key drivers, and outstanding issues. Renew Sustain Energy Rev 2018;90:402–11.
[10] Anderson WW. Resilience assessment of islanded renewable energy microgrids. Technical report, Naval Postgraduate School; 2020.
[11] Aros-Vera F, Gillian S, Rehmar A, Rehmar L. Increasing the resilience of critical infrastructure networks through the strategic location of microgrids: A case study of hurricane maria in puerto rico. Int J Disaster Risk Reduct 2021;55:102055.
[12] Su J, Li Z, Jin A. Practical model for optimal carbon control with distributed energy resources. IEEE Access 2021;9:161603–12.
[13] Security Committee I. Presidential Policy Directive 21 Implementation: An Interagency Security Committee White Paper. Technical report, 2015.
[14] Ton DT, Smith MA. The U.S. department of energy's microgrid initiative. Electr J 2012.
[15] National Infrastructure Advisory Council (NIAC). Surviving a Catastrophic Power Outage: How to Strengthen the Capabilities of the Nation. Technical report, 2018.
[16] Lenhart S, Araújo K. Microgrid decision-making by public power utilities in the united States: A critical assessment of adoption and technological profiles. Renew Sustain Energy Rev 2021;139:110692.
[17] Kizito R, Liu Z, Li X, Sun K. Stochastic optimization of distributed generator location and sizing in an islanded utility microgrid during a large-scale grid disturbance. Sustain Energy Grids Netw 2021;27:100516.
[18] Baca M, Schenkman B, Hightower M. Use of advanced microgrids to support community resilience. Natural Hazards Rev 2021;22(4):05021012.
[19] Yadav M, Pal N, Saini DK. Microgrid control, storage, and communication strategies to enhance resiliency for survival of critical load. IEEE Access 2020;8:169047–69.
[20] Marnay C, Aki H, Hirose K, Kwasinski A, Ogura S, Shinji T. Japan's pivot to resilience: How two microgrids fared after the 2011 earthquake. IEEE Power Energy Mag 2015;13(3):44–57.
[21] Reed D. Project Overview - Montgomery County Microgrid. Technical report, Schneider Electric; 2014, p. 10.
[22] Thurston C. Fremont, California, fire station is first in US with solar microgrid. 2019, https://cleantechnica.com/2019/04/05/fremont-ca-fire-station-is-first-in-us-with-solar-microgrid/.
[23] Borghei M, Ghassemi M. Optimal planning of microgrids for resilient distribution networks. Int J Electr Power Energy Syst 2021;128:106682.
[24] Gilani MA, Kazemi A, Ghasemi M. Distribution system resilience enhancement by microgrid formation considering distributed energy resources. Energy 2020;191:116442.
[25] Raya-Armenta JM, Bazmohammadi N, Avina-Cervantes JG, Saez D, Vasquez JC, Guerrero JM. Energy management system optimization in islanded microgrids: An overview and future trends. Renew Sustain Energy Rev 2021;149:111327.
[26] Shezan SA, Hasan KN, Rahman A, Datta M, Datta U. Selection of appropriate dispatch strategies for effective planning and operation of a microgrid. Energies 2021;14(21):7217.
[27] Kumar S, Saket R, Dheer DK, Holm-Nielsen JB, Sanjeevikumar P. Reliability enhancement of electrical power system including impacts of renewable energy sources: a comprehensive review. IET Gener Trans Distrib 2020;14(10):1799–815.
[28] Riou M, Dupriez-Robin F, Grondin D, Le Loup C, Benne M, Tran QT. Multi-objective optimization of autonomous microgrids with reliability consideration. Energies 2021;14(15):4466.
[29] Aruna S, Suchitra D, Rajarajeswari R, Fernandez SG. A comprehensve review on the modern power system reliability assessment. Int Jof Renew Energy Res (IJRER) 2021;11(4):1734–47.
[30] Talukdar BK, Deka BC, Goswami AK. Reliability analysis of an active distribution network integrated with solar, wind and tidal energy sources. Int Trans Electr Energy Syst 2021;e13201.
[31] Myhre SF, Fosso OB, Gjerde Or, Heegaard PE. Reliability assessment of distribution systems including microgrids. 2021, arXiv preprint arXiv:2111.07674.
[32] Aslani M, Imanloozadeh A, Hashemi-Dezaki H, Hejazi MA, Nazififard M, Ketabi A. Optimal probabilistic reliability-oriented planning of islanded microgrids considering hydrogen-based storage systems, hydrogen vehicles, and electric vehicles under various climatic conditions. J Power Sources 2022;525:231100.
[33] Xie H, Teng X, Xu Y, Wang Y. Optimal energy storage sizing for networked microgrids considering reliability and resilience. IEEE Access 2019;7:86336–48.
[34] Wu R, Sansavini G. Integrating reliability and resilience to support the transition from passive distribution grids to islanding microgrids. Appl Energy 2020;272:115254.

[35] Najafi J, Peiravi A, Anvari-Moghaddam A, Guerrero JM. An efficient interactive framework for improving resilience of power-water distribution systems with multiple privately-owned microgrids. Int J Electr Power Energy Syst 2020;116:105550.
[36] Najafi J, Anvari-Moghaddam A, Mehrzadi M, Su C-L. An efficient framework for improving microgrid resilience against islanding with battery swapping stations. IEEE Access 2021;9:40008–18.
[37] Silva FJ, De La Figuera DS. A capacitated facility location problem with constrained backlogging probabilities. Int J Prod Res 2007;45(21):5117–34.
[38] Marianov V, Serra D. Location problems in the public sector. In: Facility Location: Applications and Theory. Springer; 2002.
[39] Church R, ReVelle C. The maximal covering location problem. Pap Regional Sci Assoc 1974;32(1):7–212.
[40] Holguin JP, Rodriguez DC, Ramos G. Reverse power flow (RPF) detection and impact on protection coordination of distribution systems. IEEE Trans Ind Appl 2020;56(3):2393–401.
[41] Kizito R, Li X, Sun K, Li S. Optimal distributed generator placement in utility-based microgrids during a large-scale grid disturbance. IEEE Access 2020;8:21333–44.
[42] National Climatic Data Center (NCDC). Days of Sunshine Per Year in Tennessee, https://www.currentresults.com/Weather/Tennessee/annual-days-of-sunshine.php.
[43] Murphy J. Benders, Nested Benders and Stochastic Programming: An Intuitive Introduction. Technical report, Cambridge University Engineering Department; 2013, p. 39–48.
[44] Birge JR, Louveaux F. In: Mikosch TV, Resnick SI, Robinson SM, editors. Introduction to Stochastic Programming. Second ed. New York: Springer; 2011, p. 265–76.
[45] Fu R, Feldman D, Margolis R. U.S. Solar Photovoltaic System Cost Benchmark: Q1 2018. Technical report, National Renewable Energy Laboratory; 2018.
[46] Kizito R. MS-CFLCP model data file. 2021, https://drive.google.com/file/d/16UZ_sj3NG8qwR637F5_PnYEMHamWiTib/view?usp=sharing.
[47] National Center for Environmental Information. Comparative climatic data for the United States through 2019. 2019, https://www.ncdc.noaa.gov/sites/default/files/attachments/CCD-2019New.pdf.
[48] National Renewable Energy Laboratory (NREL). PVWatts Calculator. 2016, https://pvwatts.nrel.gov/index.php.
[49] Richardson J. Solar panels do work on cloudy days. 2018, https://cleantechnica.com/2018/02/08/solar-panels-work-cloudy-days-just-less-effectively/.
[50] Tennessee Valley Authority (TVA). Tennessee valley solar calculator solar FAQs. 2016, https://www.tva.com/energy/valley-renewable-energy/solar-q-a.
[51] USEnergy Information Administration. Commercial buildings energy consumption survey (CBECS). 2012, https://www.eia.gov/consumption/commercial/data/2012/.
[52] National Climatic Data Center (NCDC). Average Annual Sunshine by State, https://www.currentresults.com/Weather/US/average-annual-state-sunshine.php.
[53] Wilson E. Commercial and residential hourly load profiles for all TMY3 locations in the United States. 2013, https://openei.org/doe-opendata/dataset/commercial-and-residential-hourly-load-profiles-for-all-tmy3-locations-in-the-united-states.
[54] Enbar N, Weng D, Klise G. Budgeting for solar PV plant operations and maintenance: Practices and pricing. Technical Report December, Electric Power Research Institute and Sandia National Laboratories; 2015.
[55] Mongird K, Fotedar V, Viswanathan V, Koritarov V, Balducci P, Hadjerioua B, Alam J. Energy Storage Technology and Cost Characterization Report. Technical report, U.S. Department of Energy (DoE); 2019.